Optimisation Of Steady Longitudinal Pull-Up Maneuver

A thesis submitted in partial fulfilment of the requirements

for the degree of Master of Technology

by

Raman

22101053

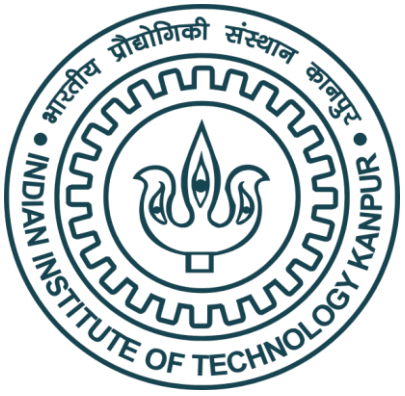

DEPARTMENT OF AEROSPACE ENGINEERING

INDIAN INSTITUTE OF TECHNOLOGY KANPUR

Feb 2023

Abstract

Name of the student: **Raman** Roll No: **22101053**

Degree for which submitted: **M.Tech** Department: **Aerospace Department**

Thesis title: **Optimisation of Steady Longitudinal Pull-up Maneuver**

Thesis supervisors: **Dr.Raghavendra P Kukillaya**

Month and year of thesis submission: **Feb 2023**

Modern aerospace power with its capability of controlling and exploiting air and space environment, has become a vital pillar in the country's national and security objectives. With the modernisation and advancements in technology, the air warfare is always evolving into new tactics and strategies. However, even today the potency of a modern day fighter aircraft in the air combat scenario becomes indispensable. It has been and will continue to be a lethal platform for delivering air power and in upholding its prowess in aerial warfare.

Fighter aircraft, since its advent, has splendidly embarked the ladder of modernisation, and a modern day fighter has evolved into a multi role platform competent enough to achieve air superiority and air supremacy. This super-manoeuvrability is attained by performing dynamic manoeuvres, which involves the airplane, at times, flying close to its operational limits. This is where the need for optimisation of the flight maneuvers comes into picture, so that we make the most efficient use of the available range of control inputs to attain the optimum performance in that particular maneuver. Optimisation also would help us paint the aircraft's operational boundary and thus would enable us to extract the best of the fighter's agility and manoeuvrability.

To optimise the entire array of flight maneuvers for a fighter aircraft in the longitudinal as well as lateral-directional plane is a formidable task. Here we initiate this task by

only focusing on the aircraft trim states and on optimising a steady coordinated pull-up maneuver in the longitudinal plane, with an intention of maximizing the pitch rate, while accounting for engine thrust constraints, AOA restrictions, structural limits, and control surface deflection limitations. With this view in mind, we have analysed two classes of airplane : one a transport class of aircraft - Hansa-3, and the other a high-AOA maneuverable fighter aircraft - F-18 HARV.

These two airplanes exhibit quite different dynamic behaviour owing to the differences in their aerodynamic, structural and propulsive designs. Hansa-3, which is designed for low-speed low-AOA flight, essentially has a linear aerodynamic model and a lower thrust capacity, whereas the F-18, designed for high-AOA maneuvers, has a relatively higher thrust capacity with the aerodynamic stability and control derivatives varying as a functionof AOA.

To obtain the dynamic response of the aircraft, we numerically integrate the six degrees of freedom (6DOF) equations of motion using MATLAB software. The specific maneuver that we study for both the aircraft is a longitudinal pull-up starting from a steady, straight and level trim state at a particular flight velocity. The goal is to negotiate a steady pull-up while maintaining velocity until the aircraft reaches the topmost inverted position. The optimization objective is to maximize the achievable steady pitch rate (minimize time) subject to the aircraft's aerodynamic and structural limitations, and the constraints on engine thrust and control surface deflections.

The results for the two aircraft demonstrate the characteristics of a classic $V - n$ diagram subject to thrust limitations. These results also help us to see how the two classes of aircraft are different in terms of their maneuverability capabilities. Using this work as the basis, we intend to explore unsteady pull-up maneuvers and rolling pull-up maneuvers in search of a more time-optimal maneuver.

Contents

List of Figures

List of Tables

Abbreviations

NAL	National Aerospace Laboratories
CG	Centre of Gravity
AOA	Angle of Attack
DOF	Degrees of Freedom
HARV	High AOA Research Vehicle

Symbols

α	Angle of attack
$\bar{c}$	Mean aerodynamic chord
β	Sideslip angle
δ_e	Elevator deflection
L	Rolling moment
M	Pitching moment
N	Yawing moment
ϕ	Body-axis roll angle
ψ	Body-axis yaw angle
ρ	Density of air
ϑ	Body-axis pitch angle
b	Wing span
C_D	Coefficient of drag
C_L	Coefficient of lift
C_m	Coefficient of pitching moment
D	Drag
g	Acceleration due to gravity
I_{xx}	Roll inertia
I_{xz}	Product of inertia in the XZ plane
I_{yy}	Pitch inertia
I_{zz}	Yaw inertia
L_f	Lift
p	Body-axis roll rate

q	Body-axis pitch rate
r	Body-axis yaw rate
S	Wing area
T	Thrust
u	Body-axis component of inertial velocity along X axis
V	Velocity
v	Body-axis component of inertial velocity along Y axis
w	Body-axis component of inertial velocity along Z axis
X	Aero-propulsive force along body axis X direction
x_{earth}	Displacement along X axis in inertial frame
Y	Aerodynamic force along body axis Y direction
y_{earth}	Displacement along Y axis in inertial frame
Z	Aerodynamic force along body axis Z direction
z_{earth}	Displacement along Z-axis in inertial frame
X_B	Body frame X axis
Y_B	Body frame Y axis
Z_B	Body frame Z axis
X_W	Wind frame X axis
Y_W	Wind frame Y axis
Z_W	Wind frame Z axis
X_I	Inertial frame X axis
Y_I	Inertial frame Y axis
Z_I	Inertial frame Z axis
C_w^B	Transformation matrix from wind frame to body frame
C_I^B	Transformation matrix from inertial frame to body frame

Chapter 1

Introduction

1.1 Background

Maneuverability and agility is one key parameter which elucidates the performance potential of a fighter aircraft. A modern day fighter is equipped with the state of the art sensors, stealth capability, powerful aero-engines, Beyond Visual Range weaponry, lift augmentation devices and Fly by Wire controls, which empowers it with lethal combat capabilities. However, when a fighter aircraft engages in a close combat with an opponent in the aerial battlefield, it is its super-maneuverability and agility which would enable it to have the better of its adversary.

It is in this context that the performance optimisation of maneuvers becomes indispensable. This would enable the aircraft to fly close to its operational limits to attain super-maneuverability and agility while at the same time making optimum utilisation of control surface and actuator deflections. To achieve this, we will have to go about optimising the steady and unsteady aircraft maneuvers, both in the longitudinal and lateral-directional plane and define an algorithm for the same.

1.2 Objective

The objective of this research work is to study, analyse and understand the aircraft dynamic responses, when it is optimised to obtain the maximum pitch rate in a steady longitudinal pull-up maneuver. Herein we study the aerodynamic models of two contrasting aircraft, Hansa-3 and F-18 HARV, when they are subject to a set of constraints in thrust factor, load factor and AOA.

1.3 Scope and Limitation

We limit our scope of study to the steady coordinated pull-up maneuvers in the longitudinal plane, and thus incorporate these steady-state conditions while solving the aircraft's 6- DOF equations of motion.

1.4 Methodology

The aerodynamic model of both Hansa-3 and F-18 are studied and their trim state analysis is carried out. The aircraft's 6-DOF dynamic and kinematic equations of motion were then numerically integrated in MATLAB to obtain the aircraft dynamic states. The pitch rate optimisation in the steady pull-up in the longitudinal plane is carried out by feeding in a cost function to be maximised in the MATLAB's *fmincon* optimiser, after setting in the constraints of thrust Factor, AOA and load factor.

1.5 Organization of the Thesis

The thesis work has been broken down in the following chapters as enumerated below:

(a) **Chapter 2** discusses the dynamic and kinematic equations of motion of an airplane, the reference frame and coordinate system used and the trim state analysis of the

aircraft longitudinal model, both in a straight and level flight condition and in the steady pull-up maneuver.

(b) **Chapter 3** analyses the aerodynamic model of Hansa-3 aircraft, its trim state condition and the dynamic behaviour when doing a steady pitch-rate-optimised pull-up maneuver.

(c) **Chapter 4** studies the aerodynamic model of F-18 HARV, its trim analysis and the aircraft behaviour when subject to pitch rate optimisation in a steady longitudinal pull-up.

(d) **Chapter 5** presents the summary of the study and concludes the work with a mention of the future scope in continuation to this study.

Chapter 2

Aircraft Dynamics and Trim Analysis

The mathematical model of the airplane describes the dynamics of flight vehicle through a set of non-linear coupled differential equations.

2.1 Assumptions

The 12 non linear differential equations defining the 6-DOF equations of motion has been formulated by considering the following assumptions [1][2]:

(a) The Earth is approximated to be flat and non-rotating and so it can be considered as the Inertial frame of reference.

(b) The flight vehicle is considered to be a rigid body and hence the CG does not move because of flexibility.

(c) The flight vehicle is considered to have 6 degrees of freedom- 3 translational and 3 rotational.

(d) The effect on mass of the aircraft due to fuel consumption is neglected i.e. $dm/dt = 0$.

(e) The inertial effect of the control surface movement on the rigid body dynamics of the aircraft is ignored.

(f) Only aerodynamic, gravitational and propulsive forces and moments are considered.

(g) The thrust is considered to be acting along the line of the body X-axis ($\alpha_t = 0$).

(h) The gravity field is assumed to be uniform.

(j) The XZ-plane is considered to be the plane of symmetry and $I_{xy} = I_{yz} = 0$.

(k) The rotation of jet engine rotors or the propeller blades is not catered for in these equations.

(I) Bending and twisting of aerodynamic surfaces is not considered and hence no additional moment because of that.

2.2 Reference Frame and Coordinate System

A reference frame is a rigid body or a set of rigidly connected points that can be used to define velocity or acceleration. Whereas a coordinate system is usually a measurement device that is attached to a reference frame to quantify the magnitude or the direction of the measured motion. The reference frame along with their coordinate system that would be useful to us in the course of this dynamic analysis are discussed as below.

(a) Body-Fixed Frame

The coordinate system of the body fixed frame is attached to the flight vehicle, with the origin fixed at the CG of the aircraft. This coordinate system rotates and translates along with the flight vehicle, with the X_B axis fixed along the longitudinal axis of the aircraft, the Y_B along the starboard wing perpendicular to X_B. The Z_B axis completes the right-hand coordinate system acting along the normal axis. The X_B and Z_B are in the aircraft symmetric axis.

(b) Inertial Frame (NED Frame)

It is a right hand coordinate system, with the X_I acting along the north, the Y_I along the east and the Z_I acting along the line of the gravity. This constitutes the NED (North-East-Down) frame, which is an inertial frame. The Newton's Laws of motion can only be applied to the inertial Frame.

(c) Wind-Fixed Frame

The Wind-fixed frame of coordinate system proves very pertinent to our dynamic analysis, as it is structured around the aerodynamic forces and the aerodynamic angles. The origin is again at the CG of the flight vehicle and the X_W is oriented towards the local flight velocity, V_∞. The Z_W acts perpendicularly along the air- craft plane of symmetry. The Y_W is along the starboard wing perpendicular to the symmetric plane.

2.2.1 Coordinate Transformations

The coordinate system transformation helps us to represent the velocity or acceleration observed from a particular reference frame into a different reference frame coordinate system. The transformation that would be required for our analysis are mentioned below.

(a) Wind-Frame to Body-Fixed Frame

The transformation from the wind frame system to the body frame would require us to do two rotations of $-\beta$ and α along the Z_W axis and the intermediate Y axis respectively. The transformation matrix is given below. In order to achieve the reverse transformation, i.e. from body frame to wind frame we need to transpose the transformation matrix. The Fig2.1helps us visualize the relation of body-axis coordinate system to the wind-axis through the aerodynamic angles.

$$C_w^B = \begin{bmatrix} \cos\alpha\cos\beta & -\cos\alpha\sin\beta & -\sin\alpha \\ \sin\beta & \cos\beta & 0 \\ \sin\alpha & -\sin\alpha\sin\beta & \cos\alpha \end{bmatrix}$$

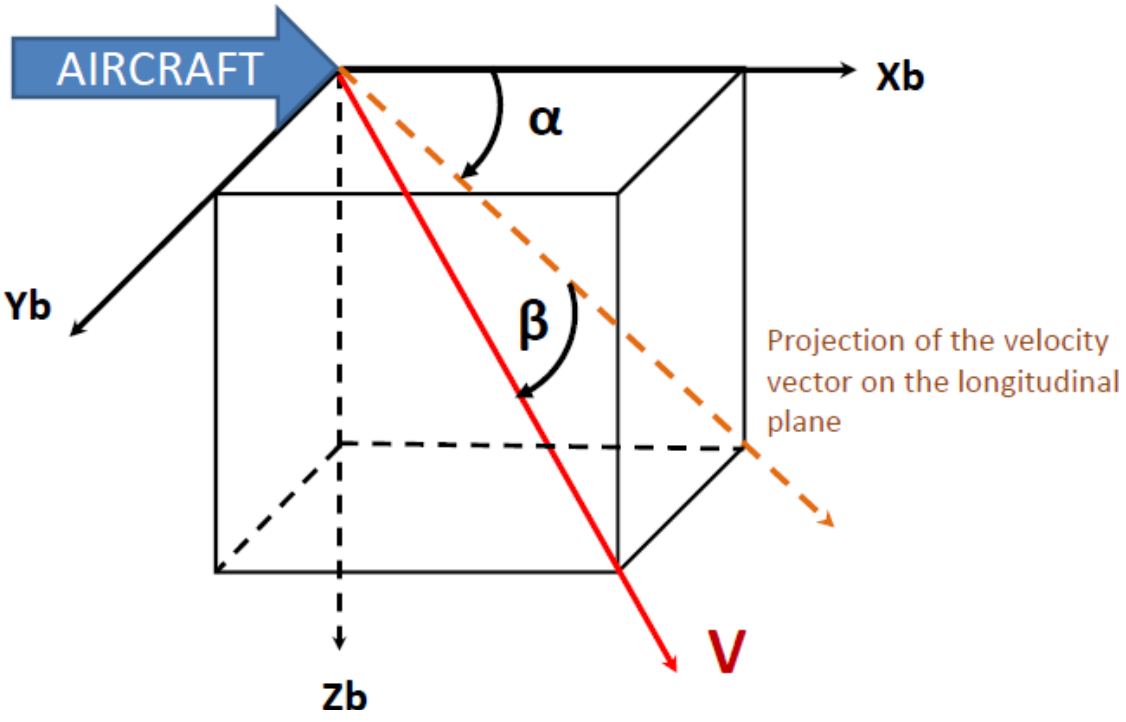

FIGURE 2.1: Aerodynamic angles relating body-axis to wind-axis

(b) Inertial-Frame to Body-Fixed Frame

The transformation from the Inertial frame to the Body-frame can be achieved by doing three rotations of ψ, ϑ and ϕ along the Z_I axis, intermediate Y axis and the second intermediate X axis respectively. The transformation matrix is given below.

$$C^B = \begin{bmatrix} \cos\psi\cos\vartheta & \sin\psi\cos\vartheta & -\sin\vartheta \\ -\sin\psi\cos\varphi & \sin\psi\sin\vartheta\sin\varphi + \cos\psi\cos\varphi & \cos\vartheta\sin\varphi \\ \cos\psi\sin\vartheta\cos\varphi + \sin\psi\sin\varphi & \sin\psi\sin\vartheta\cos\varphi - \cos\psi\sin\varphi & \cos\vartheta\cos\varphi \end{bmatrix}$$

2.3 Equations of Motion

The mathematical model of an aircraft can be represented by the following set of coupled non-linear differential equations which can be numerically integrated to obtain the dynamic states of the aircraft starting from an initial condition and subject to some external forces and moments.

(a) Translational Dynamics

The coupled non-linear translational dynamics equations represent the relation between the acceleration in body axis system and the aero-propulsive and gravitational forces acting on the vehicle as represented in Equations2.1. Here, the thrust force is considered to be acting in line with the X-axis, so the X is the aero-propulsive force.

$$\begin{aligned} \dot{u} &= \frac{X}{m} - wq - vr - g\sin\vartheta \\ \dot{v} &= \frac{Y}{m} - ur + wp + g\cos\vartheta\sin\phi \\ \dot{w} &= \frac{Z}{m} - vp + uq + g\cos\vartheta\cos\phi \end{aligned} \tag{2.1}$$

(b) Rotational Dynamics

These equations relate the body axis angular accelerations to the aerodynamic moments as shown in Equations2.2

$$\begin{aligned} \dot{p} &= \frac{1}{I_{xx}}[(I_{yy} - I_{zz})qr + I_{xz}pq + L] \\ \dot{q} &= \frac{1}{I_{yy}}[(I_{zz} - I_{xx})pr + I_{xz}(p^2 - r^2) + M] \\ \dot{r} &= \frac{1}{I_{zz}}[(I_{xx} - I_{yy})pq + I_{xz}qr + N] \end{aligned} \tag{2.2}$$

(c) Rotational Kinematics

The kinematic equations represent the relation between the Euler angle rates and the body axis rates of the flight vehicle as given by Equations2.3

$$\begin{aligned} \dot{\psi} &= q\sin\phi + r\cos\phi\cos\vartheta \\ \dot{\vartheta} &= q\cos\phi - r\sin\phi \\ \dot{\phi} &= p + \tan\vartheta(q\sin\phi + r\cos\phi) \end{aligned} \tag{2.3}$$

(d) Translational Kinematics

It represents the relation of the translational motion to the body axis flight velocities as given by Equations2.4

$$\begin{aligned}
\dot{x}_{\text{earth}} &= u\cos\psi\cos\vartheta + v(\cos\psi\sin\vartheta\sin\phi - \sin\psi\cos\phi) + w(\cos\psi\sin\vartheta\cos\phi + \sin\psi\sin\phi)\\
\dot{y}_{\text{earth}} &= u\sin\psi\cos\vartheta + v(\sin\psi\sin\vartheta\sin\phi + \cos\psi\cos\phi) + w(\sin\psi\sin\vartheta\cos\phi - \cos\psi\sin\phi)\\
\dot{z}_{\text{earth}} &= -u\sin\vartheta + v\cos\vartheta\sin\phi + w\cos\vartheta\cos\phi
\end{aligned} \tag{2.4}$$

2.4 Longitudinal Model

The aircraft longitudinal model focuses on the motion of an airplane in the XZ-longitudinal plane and its states can be defined as tabulated in Table2.1. When the values of the states given in Table2.1is applied in Equations2.1-2.4, we obtain the Equation2.5.

TABLE 2.1: States and state-derivatives for a longitudinal model

State	Value	State-Derivative	Value
u	Variable	$\dot{u}$	Variable
v	0	$\dot{v}$	0
w	Variable	$\dot{w}$	Variable
p	0	$\dot{p}$	0
q	Variable	$\dot{q}$	Variable
r	0	$\dot{r}$	0
γ	Variable	$\dot{\gamma}$	$q - \dot{\alpha}$
ϕ	0	$\dot{\phi}$	0
ψ	0	$\dot{\psi}$	0
ϑ	Variable	$\dot{\vartheta}$	q
α	Variable	$\dot{\alpha}$	Variable
β	0	$\dot{\beta}$	0

$$\begin{aligned}
\dot{u} &= \frac{X}{m} - wq - g\sin\vartheta\\
\dot{w} &= \frac{Z}{m} + uq + g\cos\vartheta\\
\dot{q} &= \frac{M}{I_{yy}}\\
\dot{\vartheta} &= q
\end{aligned} \tag{2.5}$$

$$\begin{aligned}
\dot{x}_{\text{earth}} &= u\cos\vartheta + w\sin\vartheta\\
\dot{z}_{\text{earth}} &= -u\sin\vartheta + w\cos\vartheta
\end{aligned}$$

The translational dynamics equations given as the first two equations in Equations2.5can be converted into the wind axis system and can be written as Equation2.6. Here, the lift, drag and moment can be defined as given by Equation2.7.

$$\begin{aligned}
\dot{V} &= -\frac{D}{m} - g\sin(\vartheta - \alpha) + \frac{T}{m}\cos\alpha \\
\dot{\alpha} &= -\frac{L_f}{mV} + \frac{g}{V}\sin(\vartheta - \alpha) + q - \frac{T}{mV}\sin\alpha \\
\dot{q} &= \frac{M}{I_{yy}} \\
\dot{\vartheta} &= q \\
\dot{x}_{\text{earth}} &= u\cos\vartheta + w\sin\vartheta \\
\dot{z}_{\text{earth}} &= -u\sin\vartheta + w\cos\vartheta
\end{aligned} \tag{2.6}$$

$$\begin{aligned}
L_f &= \frac{1}{2}\rho(V)^2 S C_L \\
D &= \frac{1}{2}\rho(V)^2 S C_D \\
M &= \frac{1}{2}\rho(V)^2 S\bar{c} C_m
\end{aligned} \tag{2.7}$$

The coefficients of lift, drag and moment can be defined as :

$$\begin{aligned}
C_L &= C_{L_0} + C_{L_\alpha}\alpha + C_{L_q}\frac{q\bar{c}}{2V} + C_{L_{\delta e}}\delta e \\
C_D &= C_{D_0} + C_{D_\alpha}\alpha + C_{D_q}\frac{q\bar{c}}{2V} + C_{D_{\delta e}}\delta e \\
C_m &= C_{m_0} + C_{m_\alpha}\alpha + C_{m_q}\frac{q\bar{c}}{2V} + C_{m_{\delta e}}\delta e
\end{aligned} \tag{2.8}$$

2.5 Trim Analysis

The trim state of an airplane is defined as that state when all the forces and moments are considered to be balanced. Here in this context we analyse two such cases of trim flight in the longitudinal plane. One a steady, straight and level maneuver and the other a steady coordinated longitudinal pull-up maneuver. Each of these cases are elaborately discussed below.

2.5.1 Steady, Straight and Level

The dynamic states of a flight in a steady, straight and level trim condition is given by the Table2.2. The first four equations given in Equation2.1-2.4reduces to the Equation2.9 when we feed in the values given in this Table2.2.

TABLE 2.2: States and state-derivatives in a steady, straight and level trim flight

State	Value	State-Derivative	Value
V	Constant	$\dot{V}$	0
α	α_{trim}	$\dot{\alpha}$	0
β	0	$\dot{\beta}$	0
p	0	$\dot{p}$	0
q	0	$\dot{q}$	0
r	0	$\dot{r}$	0
γ	0	$\dot{\gamma}$	0
ϑ	$\alpha_{\mathbf{trim}}$	$\dot{\vartheta}$	0
ϕ	0	$\dot{\phi}$	0
ψ	0	$\dot{\psi}$	0

$$\begin{aligned} L_f &= W \\ T &= D \\ M &= 0 \end{aligned} \tag{2.9}$$

2.5.2 Steady, Coordinated Longitudinal Pull-up

A steady, coordinated longitudinal pull-up is a symmetric maneuver carried out in the vertical XZ-plane where the airplane initiates the maneuver from a straight and level, trimmed flight condition as defined by Equations2.9. The specific maneuver that we analyse includes portion in which the flight path angle varies from $\gamma = 0$ deg to $\gamma = 180$ deg inverted state. The states for this maneuver is shown in the Table2.3.

TABLE 2.3: States and state-derivatives in a steady, longitudinal pull-up

State	Value	State-Derivative	Value
u	Variable	$\dot{u}$	0
v	0	$\dot{v}$	0
w	Variable	$\dot{w}$	0
p	0	$\dot{p}$	0
q	Constant	$\dot{q}$	0
r	0	$\dot{r}$	0
γ	Variable	$\dot{\gamma}$	$q - \dot{\alpha}$
ϕ	0	$\dot{\phi}$	0
ψ	0	$\dot{\psi}$	0
ϑ	Variable	$\dot{\vartheta}$	q
α	Variable	$\dot{\alpha}$	Variable
β	0	$\dot{\beta}$	0

When the trim values of Table2.3are fed in the Equations2.6, we obtain the Equation 2.10.

$$\dot{\alpha} = \left[-\frac{\rho V S}{2m} \left(C_{L_0} + C_{L_\alpha}\alpha + C_{L_q}\frac{q\bar{c}}{2V} \right) + \left(C_{D_0} + C_{D_\alpha}\alpha + C_{D_q}\frac{q\bar{c}}{2V} \right)\tan\alpha \right]$$

$$+ \frac{\rho V S}{2m} \underbrace{\left(C_{m_0} + C_{m_\alpha}\alpha + C_{m_q}\frac{q\bar{c}}{2V} \right)\left(C_{L_{\delta_e}} + C_{D_{\delta_e}}\tan\alpha \right)}_{C_{m_{\delta_e}}} + \frac{g\cos\vartheta}{V\cos\alpha} + q$$

$$\dot{x} = V\cos\alpha\cos\vartheta + V\sin\alpha\sin\vartheta \tag{2.10}$$

$$\dot{z} = -V\cos\alpha\sin\vartheta + V\sin\alpha\cos\vartheta$$

$$\dot{\vartheta} = q$$

In a steady longitudinal pull-up the pitching moment coefficient C_m becomes 0. This gives us the elevator deflection δ_e in this maneuver as in Equation2.11.

$$\delta e = -\frac{C_{m_0} + C_{m_\alpha}\alpha + C_{m_q}\frac{q\bar{c}}{2V}}{C_{m_{\delta e}}} \tag{2.11}$$

The velocity in a steady pull-up is constant as brought out in Table2.3, which gives us the thrust requirement as given in Equation2.12.

$$T = \frac{D + W\sin(\vartheta - \alpha)}{\cos\alpha} \tag{2.12}$$

Chapter 3

Steady Longitudinal Pull-up Analysis : Hansa-3

The Hansa-3 variant chosen for this dynamic analysis is an all-composite low-wing conventional 2 seater trainer aircraft which is mainly employed for flying training and adventure sport flying. It is a single engine aircraft manufactured by National Aerospace Laborato- ries (NAL), India and equipped with primary controls as aileron, rudder and elevator and secondary controls as flaps and trim tabs. The objective behind selecting this aircraft is to study the pull-up optimisation for an aircraft having a linear aerodynamic model.

3.1 Technical Specifications

(a) Control Surface Limits

TABLE 3.1: Control surface limits.

Control Surface	Symbol	Positional Limits
Rudder	δr	-30°, 30°
Elevator	δe	-30°, 25°
Aileron	δa	-20°, 20°

(b) Aircraft Characteristics

The geometric parameters of the aircraft is given in Table3.2[3][4].

TABLE 3.2: Aircraft characteristics.

Parameter	Symbol	Value
Mass	m	750 kg
Wing Span	b	10.47 m
Aspect Ratio	AR	8.8
Oswald Efficiency Factor	e	0.7885
Mean Aerodynamic Chord	$\bar{c}$	1.21 m
Wing Area	S	12.47 m^2
Pitch Inertia	I_{yy}	907 kg-m^2
Yaw Inertia	I_{zz}	1680 kg-m^2
Roll Inertia	I_{xx}	873 kg-m^2
Product of Inertia	I_{xz}	1144 kg-m^2

3.2 Aerodynamic Model

The aerodynamic modelling of the airplane is primarily concerned with the development of mathematical models to describe the aerodynamic forces and moments acting on the aircraft as a function of various independent variables. The aerodynamic characteristics of each aircraft is unique and can be represented as a function of different state and control variables and its aerodynamic stability and control derivatives as represented by set of Equations3.1. Since we are focusing on longitudinal dynamic maneuvers, only the longitudinal aerodynamic model is used [3] [5].

$$\begin{aligned} C_L &= C_{L_0} + C_{L_\alpha}\alpha + C_{L_q}\frac{q\bar{c}}{2V} + C_{L_{\delta e}}\delta e \\ C_D &= C_{D_0} + C_{D_\alpha}\alpha + C_{D_{\delta e}}\delta e \\ C_m &= C_{m_0} + C_{m_\alpha}\alpha + C_{m_q}\frac{q\bar{c}}{2V} + C_{m_{\delta e}}\delta e \end{aligned} \tag{3.1}$$

The static variation of the coefficient of lift C_L, coefficient of drag C_D and the coefficient of pitching moment C_m with the angle of attack α is graphically represented below. The

restricted static longitudinal aerodynamic model given as

$$\begin{aligned} C_L &= C_{L_o} + C_{L_\alpha}\alpha \\ C_D &= C_{D_o} + C_{D_\alpha}\alpha \\ C_m &= C_{m_o} + C_{m_\alpha}\alpha \end{aligned} \tag{3.2}$$

(a) Lift Coefficient

The variation of coefficient of lift C_L with the angle of attack for a range of α from -2 deg to 8 deg is linear due to its constant slope C_{L_α} across the entire range of α. The stall angle of attack is marked in the plot as $\alpha = 6$ deg [6]. The C_{L_o} can be interpolated from the plot as 0.354.

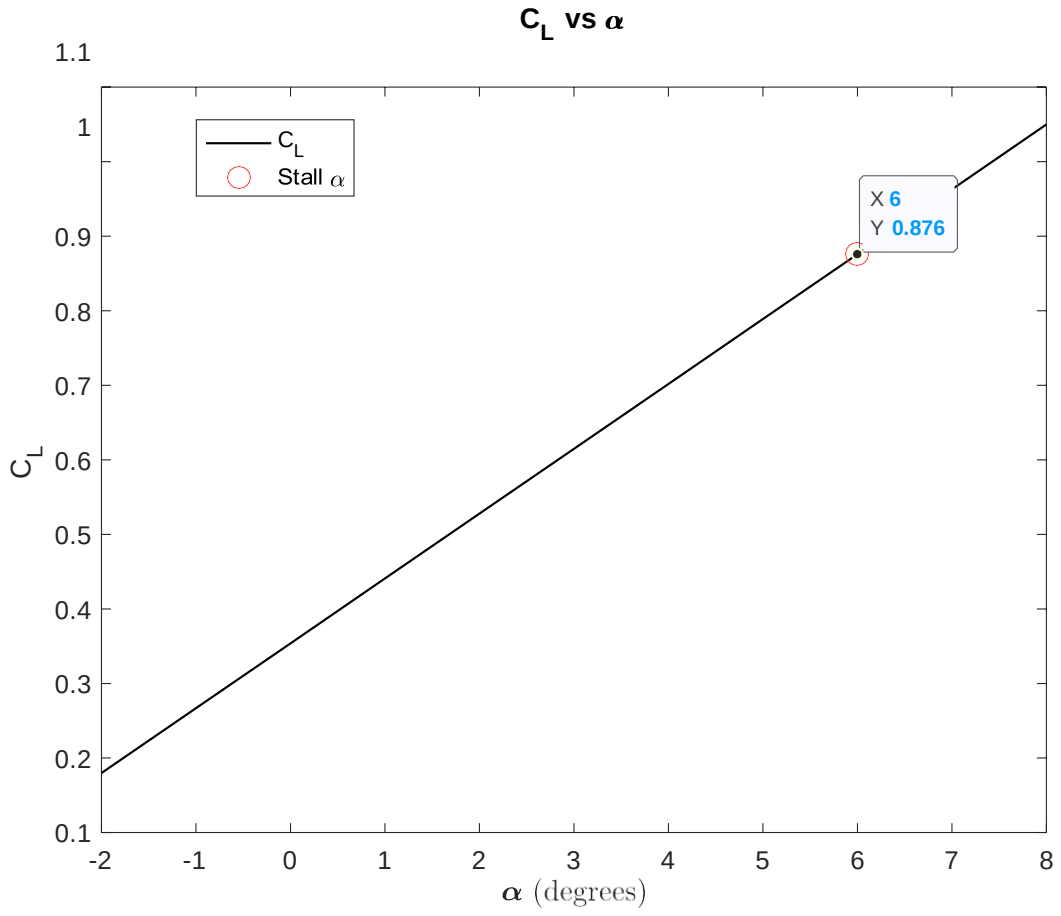

FIGURE 3.1: Variation of C_L vs α

(b) Drag Coefficient

The variation of coefficient of drag C_D with the angle of attack for a range of α from -2 deg to 8 deg is linear due to its constant slope C_{D_α} across the entire range of α and the C_{D_0} is 0.036.

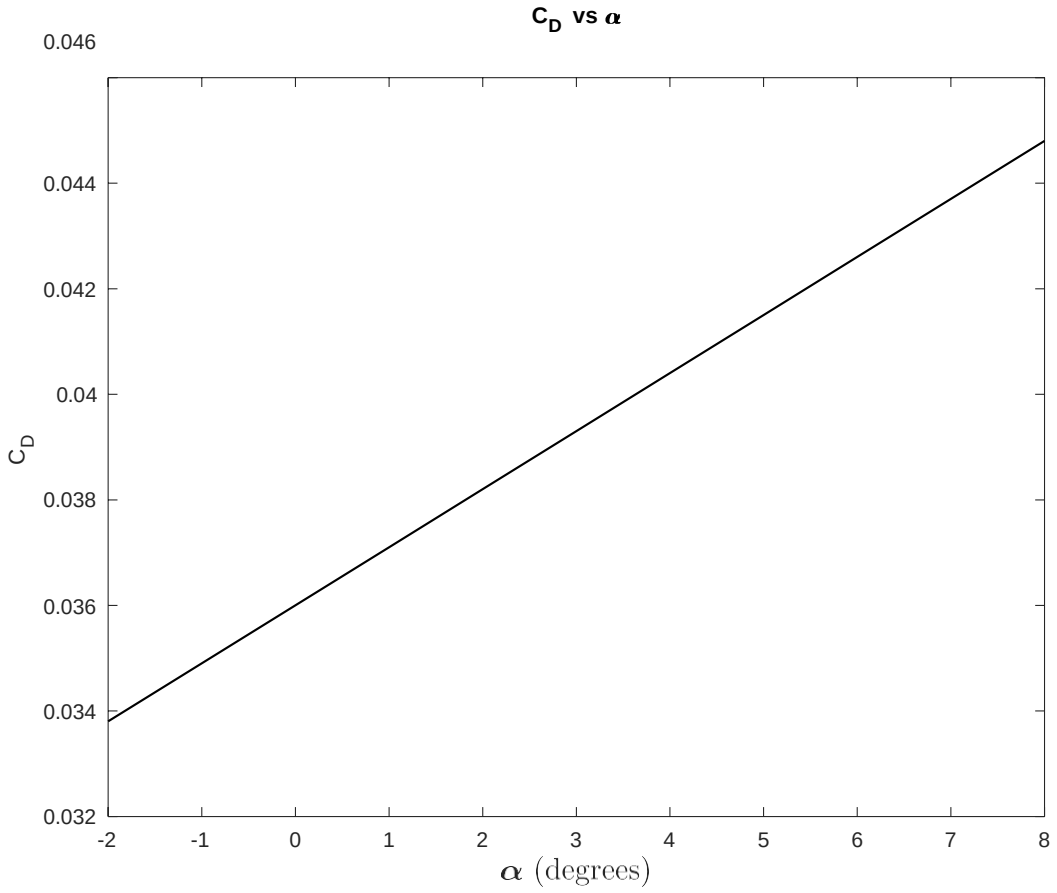

FIGURE 3.2: Variation of C_D vs α

(c) Moment Coefficient

The variation of coefficient of pitching moment C_m with the angle of attack for a range of α from -2 deg to 8 deg is linear due to its constant slope C_{m_α} across the entire range of α and the C_{m_0} can be seen from the plot as 0.052.

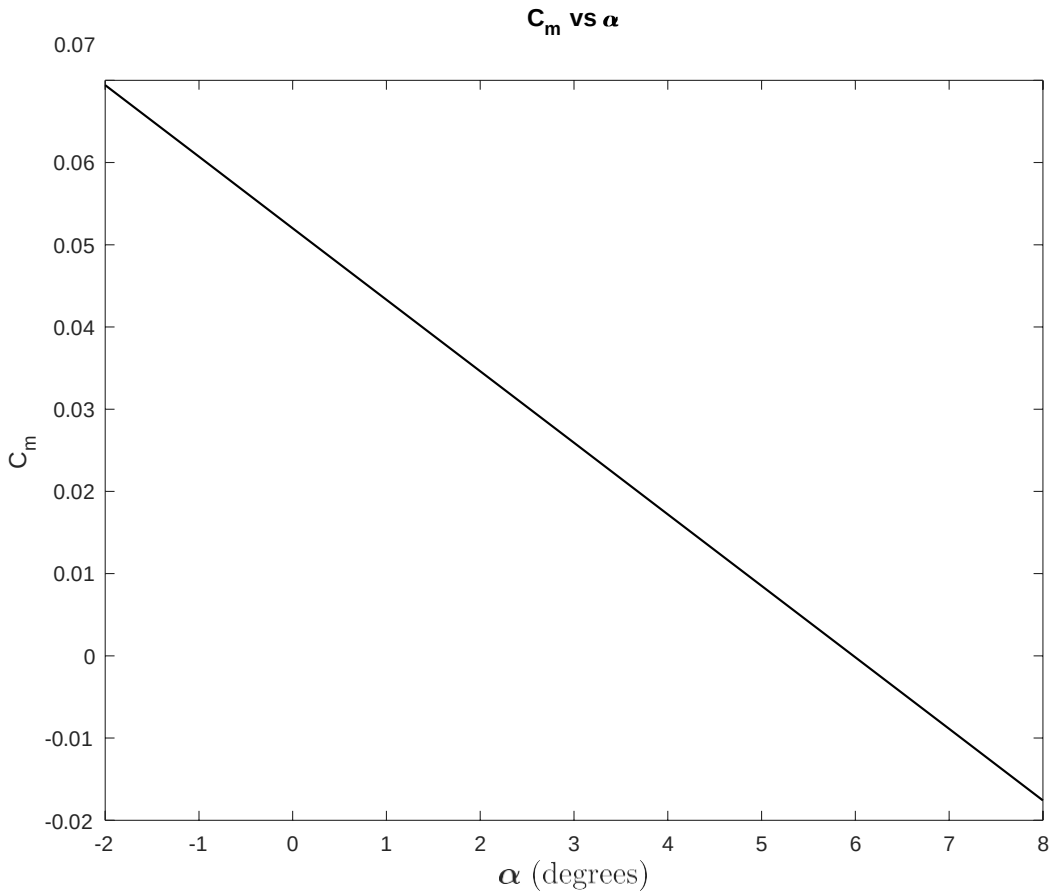

FIGURE 3.3: Variation of C_m vs α

3.3 Assumptions

The mathematical model of Hansa-3 has constant aerodynamic parameters across the entire range of α and hence the study on its pitching characteristics in the longitudinal plane becomes intriguing. However, this analysis has been made by considering a few assumptions as stated below:

(a) The Hansa-3 aircraft has a maximum power rating of 85 kW from its Bombardier Rotax 914 F3 turbocharged aero-engine [6]. However, here we have considered a limiting thrust factor ($TF = T_{max}/W$) of 1.15 for setting the thrust constraint in the optimisation problem. Although this is unrealistic, but in order to make the aircraft perform a complete inverted-loop maneuver, this gross assumption was necessary.

(b) The aircraft in a clean configuration has a stall speed of 33.4 m/s which roughly corresponds to α = 6 deg [6]. Again, it has a maximum speed of 61 m/s at sea level altitude (ρ = 1.225 kg/m^3) at α = -1.5 deg as per the original power rating of the 85 kW aero-engine. These limits for AOA have been considered while setting the constraints in the problem statement.

(c) The load factor (n) has been approximated to be bound within the range $-1 \leq n \leq 4$ and the same has been used to set the constraint boundaries in the problem.

(d) The maximum all up weight ($W = m * g$) has been considered for defining the problem statement, where mass of the aircraft is m = 750 kg and acceleration due to gravity is g = 9.81 m/s^2.

(e) Sea level altitude has been considered for calculating the air density ρ = 1.225 kg/m^3 for the entire computation.

3.4 Trim Analysis : Steady, Straight and Level

In this trim state, the aircraft is in a straight, steady and level flight condition, flying at a constant velocity and AOA governed by the following equations of motion

$$\begin{aligned} L_f &= W \\ T &= D \\ M &= 0 \end{aligned} \tag{3.3}$$

The steady state level trim analysis on the Hansa-3 aircraft has been carried for two flight velocities near the lower and upper speed bounds as illustrated below in two separate cases. For any specific flight velocity, we solve the three equations given by Equation3.3 to obtain the required control inputs, i.e. elevator (δ_e) and thrust (T). These in turn are fed as input into the flight simulation to get the plots shown in Fig3.4-3.5. In the flight simulation, the states are obtained by numerical integration of the Equations2.6using the fourth order Runge Kutta method in MATLAB.

3.4.1 Case I: Velocity (V) = 40 m/s

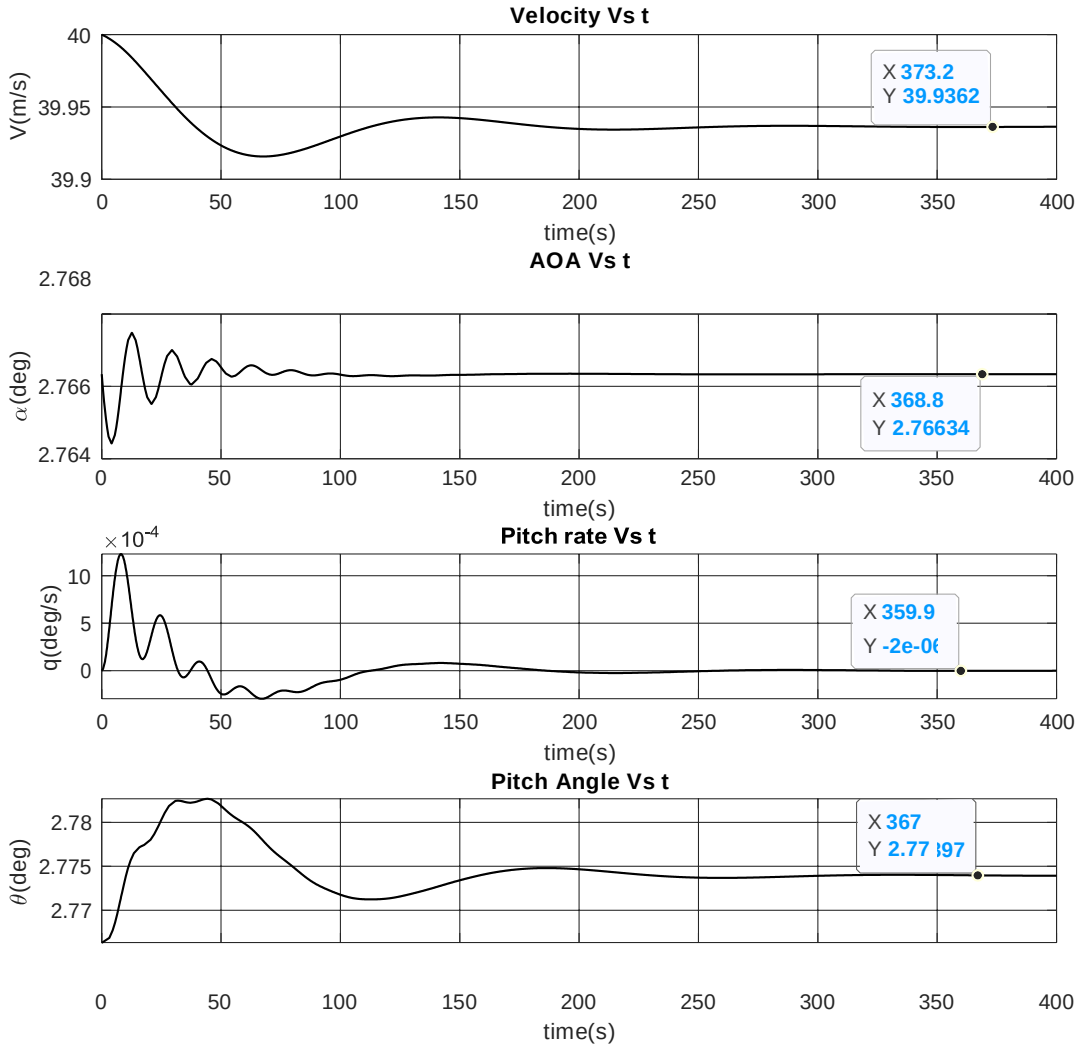

FIGURE 3.4: Velocity, AOA, pitch rate and pitch angle at level trim state

The dynamic response of the airplane when it is trimmed at straight and level condition at flight velocity V = 40 m/s can be visualized from the Fig3.4. The velocity, AOA, pitch rate and the pitch angle settles down at V = 39.96 m/s, α = 2.7 deg, q = 0 deg/s and ϑ = 2.77 deg respectively. The control inputs corresponding to the level trim state are elevator δ_e = 1.58 deg and thrust T = 484.85 N.

3.4.2 Case II: Velocity (V) = 60 m/s

Similarly, the response of the airplane when it is trimmed at flight velocity V = 60 m/s can be seen in its states as graphically represented in Fig3.5. The velocity, AOA, pitch rate and the pitch angle settles down at V = 60.05 m/s, $\alpha = -1.81$ deg, $q = 0$ deg/s and $\vartheta = -1.2$ deg respectively. The control inputs corresponding to the level trim state are elevator $\delta_e = 3.5$ deg and thrust T = 999.35 N.

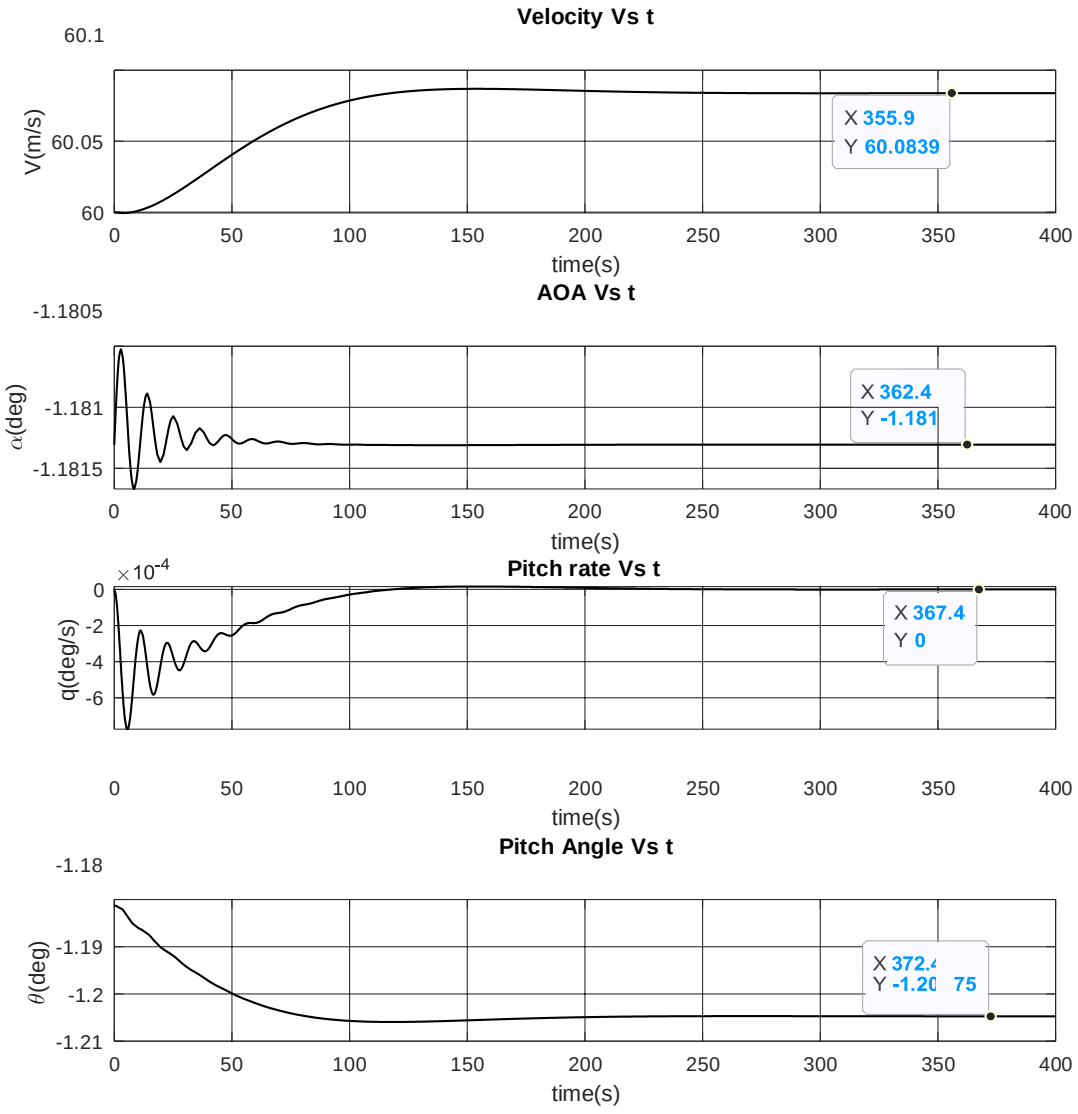

FIGURE 3.5: Velocity, AOA, pitch rate and pitch angle at level trim state

3.5 Trim Analysis : Steady Longitudinal Pull-up

A steady coordinated longitudinal pull-up is a symmetric maneuver carried out in the vertical XZ-plane where the airplane initiates the maneuver from a straight and level, trimmed flight condition and the flight path angle varies from γ = 0 deg to γ = 180 deg inverted state. Our point of interest is the dynamic response of the airplane till it settles down in the γ = 180 deg state in the least possible time, all the while maintaining a steady pitch rate. The steady state dynamic and kinematic equations governing this maneuver is shown below in Equation3.4. The airplane states are thereafter obtained by numerical integration of these equations using fourth order Runge Kutta method in MATLAB.

$$\begin{aligned}
\dot{\alpha} &= \left[-\frac{\rho V S}{2m} \left(C_{L_0} + C_{L_\alpha}\alpha + C_{L_q}\frac{q\bar{c}}{2V} \right) + \left(C_{D_0} + C_{D_\alpha}\alpha \right) \tan\alpha \right] \\
&\quad + \frac{\rho V S}{2m} \frac{\left(C_{m_0} + C_{m_\alpha}\alpha \right)\left(C_{L_{\delta_e}} + C_{D_{\delta_e}} \tan\alpha \right)}{C_{m_{\delta_e}}} + \frac{g\cos\vartheta}{V\cos\alpha} + q \\
\dot{x} &= V\cos\alpha\cos\vartheta + V\sin\alpha\sin\vartheta \qquad (3.4) \\
\dot{z} &= -V\cos\alpha\sin\vartheta + V\sin\alpha\cos\vartheta \\
\dot{\vartheta} &= q
\end{aligned}$$

3.5.1 Pitch Rate Optimisation

Optimization is a process that aims to find the most favorable solution for maximizing or minimizing a cost function while accounting for various constraints. In our problem statement, we define the cost function as the negative square of the pitch rate (q), aiming to get the maximum possible steady pitch rate in the pull-up maneuver, where the flight path angle varies from γ = 0 deg to γ = 180 deg. Here the constraints that we set are thrust factor ceiling, angle of attack limitation and maximum load factor attainable.

To solve this optimization problem, we have used MATLAB's *fmincon* function, which employs the gradient descent algorithm to arrive at the maximum possible pitch rate within the bounds of the set constraints. The optimisation design for this problem statement is illustrated in Fig3.6and Table4.3

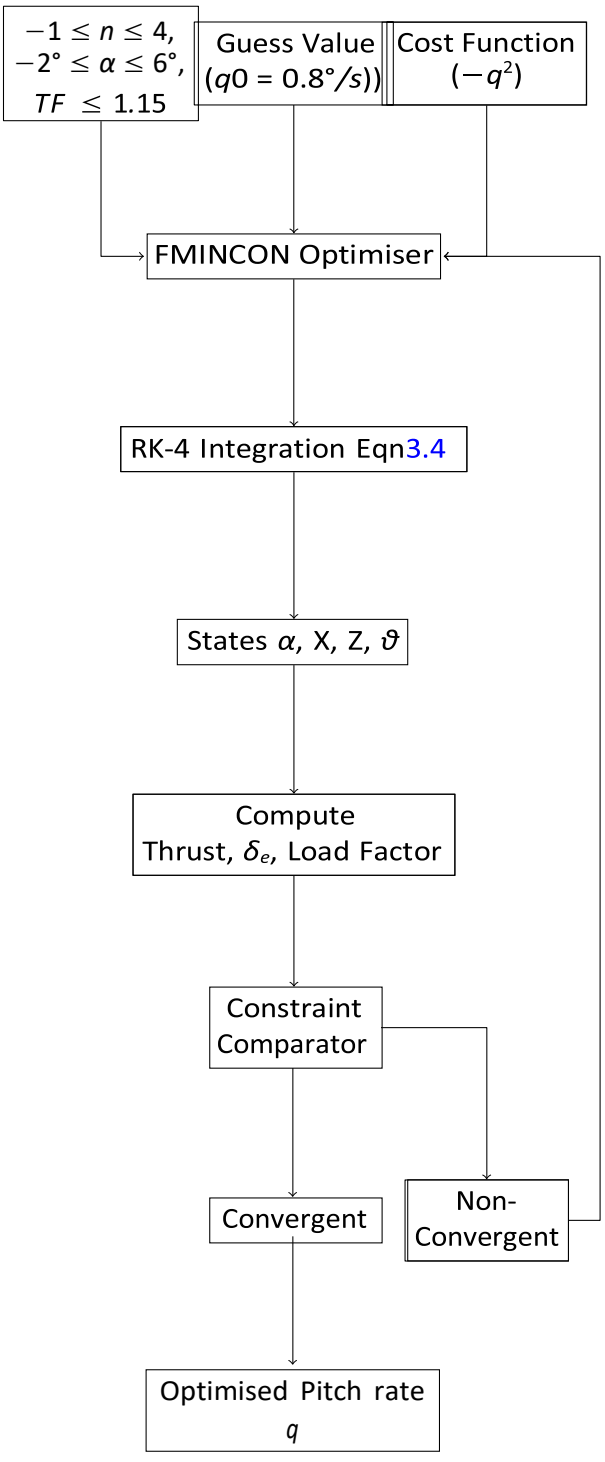

FIGURE 3.6: Optimisation process flow chart

TABLE 3.3: Pitch rate optimisation problem design

Cost Function	$-q^2$
Guess Value	$0.8\ °/s$
Constraints	**Limits**
Thrust Factor	1.15
AOA (α)	$-2° \leq \alpha \leq 6°$
Load factor(n)	$-1 \leq n \leq 4$

3.5.2 Case I: Velocity (V) = 60 m/s

The steady pull-up pitch rate optimisation is first carried out for a flight velocity of V = 60 m/s as per the design chalked out in Table3.3. The obtained states from the airplane dynamics are then plotted graphically below. Herein, we initially applied all the constraints of thrust factor, AOA and load factor to the optimisation algorithm. Thereafter we alleviated them, one at a time, as and when they were hitting the limit so as to check the dynamic responses with each of these constraints hitting their tolerance ceiling values.

(a) Limiting Constraint : Thrust Factor

The Fig3.7shows the variation of AOA, Thrust factor, load factor, elevator deflection and flight path angle γ with time, wherein we can see that the limiting factor in our pursuit to obtain the optimised pitch rate in the pull-up maneuver is the thrust factor hitting the ceiling limit of 1.15. The maximum optimised steady pitch rate in this case is q = 0.39 deg/s.

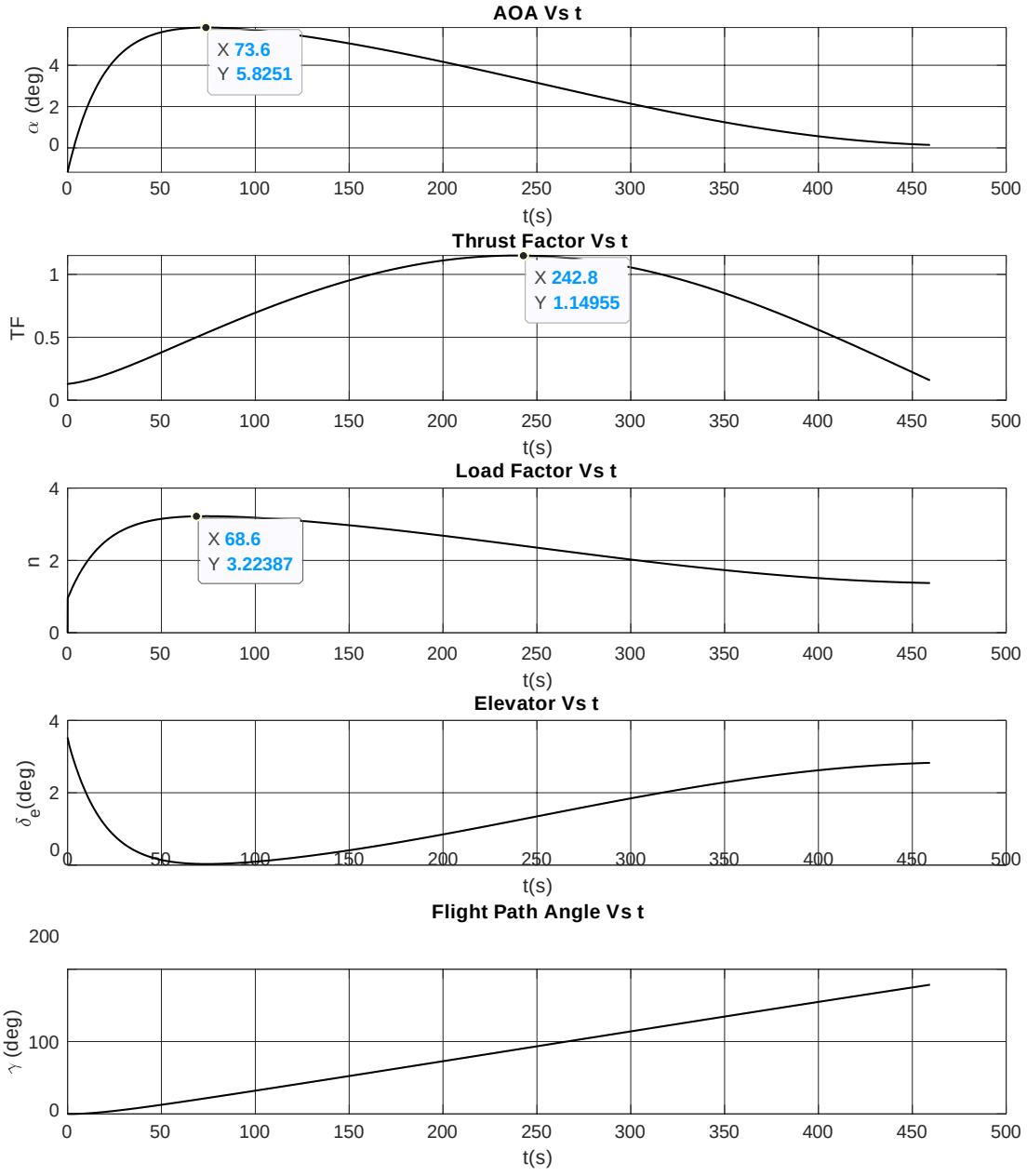

FIGURE 3.7: Variation of AOA, Thrust factor, Load factor, elevator and flight path angle with time

(b) Limiting Constraint : AOA α

If we dilute the limiting constraint of thrust factor and only apply load factor and AOA restrictions to the optimisation algorithm, we obtain the results as highlighted graphically in the Fig3.8. Here, we see that the optimised pitch rate q = 0.40 deg/s slightly increases from the previous case, and the maximum limit of AOA α= 6 deg

act as the restricting factor.

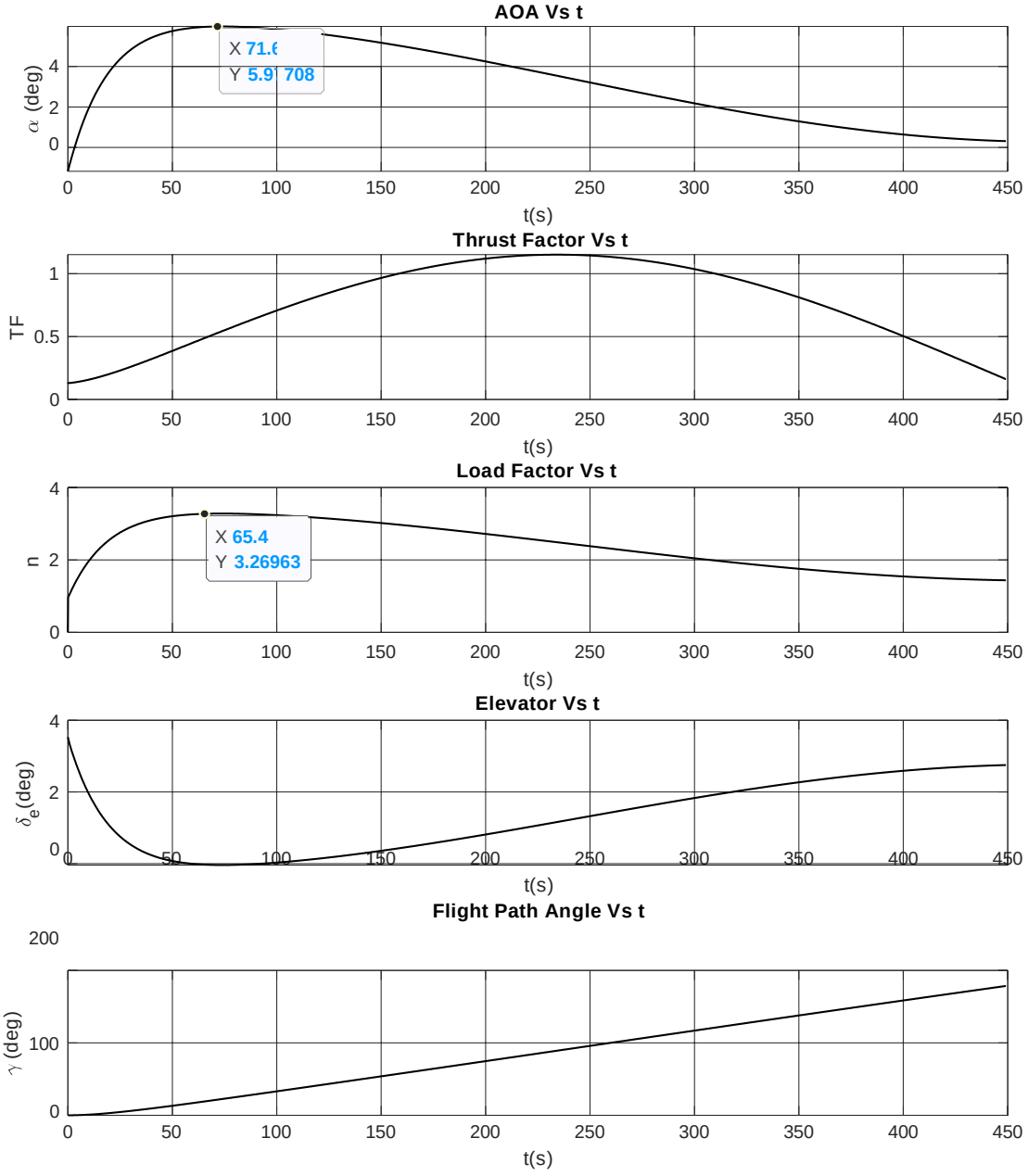

FIGURE 3.8: Variation of AOA, Thrust factor, Load factor, elevator and flight path angle with time

(c) Limiting Constraint : Load Factor

Again if we do away with the AOA restriction on the constraint definition in the optimisation problem, the pitch rate gets furthermore enhanced to q = 0.53 deg/s,

within the bound of the limiting load factor of n = 4. The plots of the dynamic responses in this case is brought out in Fig3.9.

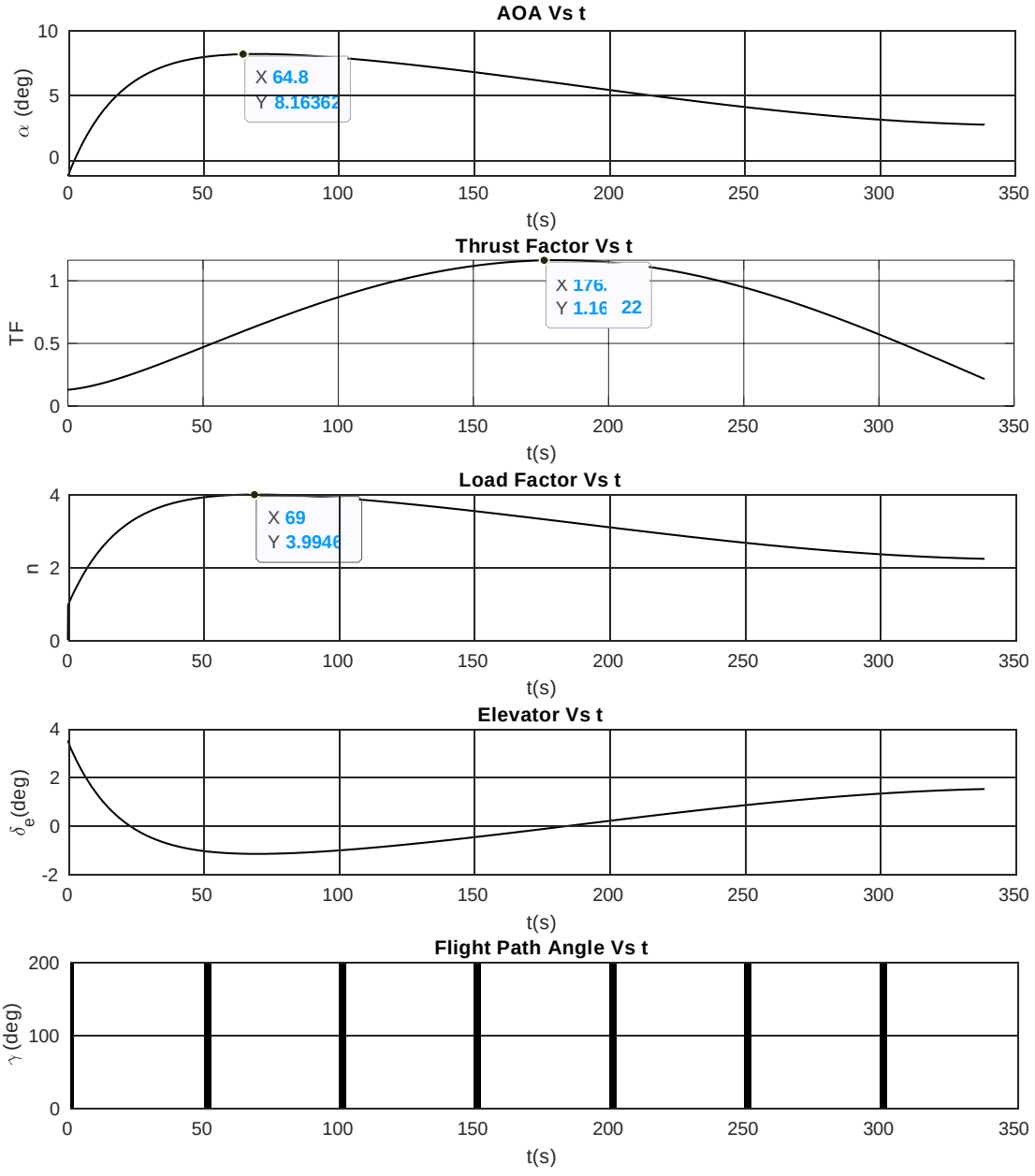

FIGURE 3.9: Variation of AOA, Thrust factor, Load factor, elevator and flight path angle with time

(d) Flight Path Trajectory

The plot in Fig3.10, shows a comparative view of the aircraft profile in a pull-up maneuver at different pitch rates and at a velocity of V = 60 m/s.

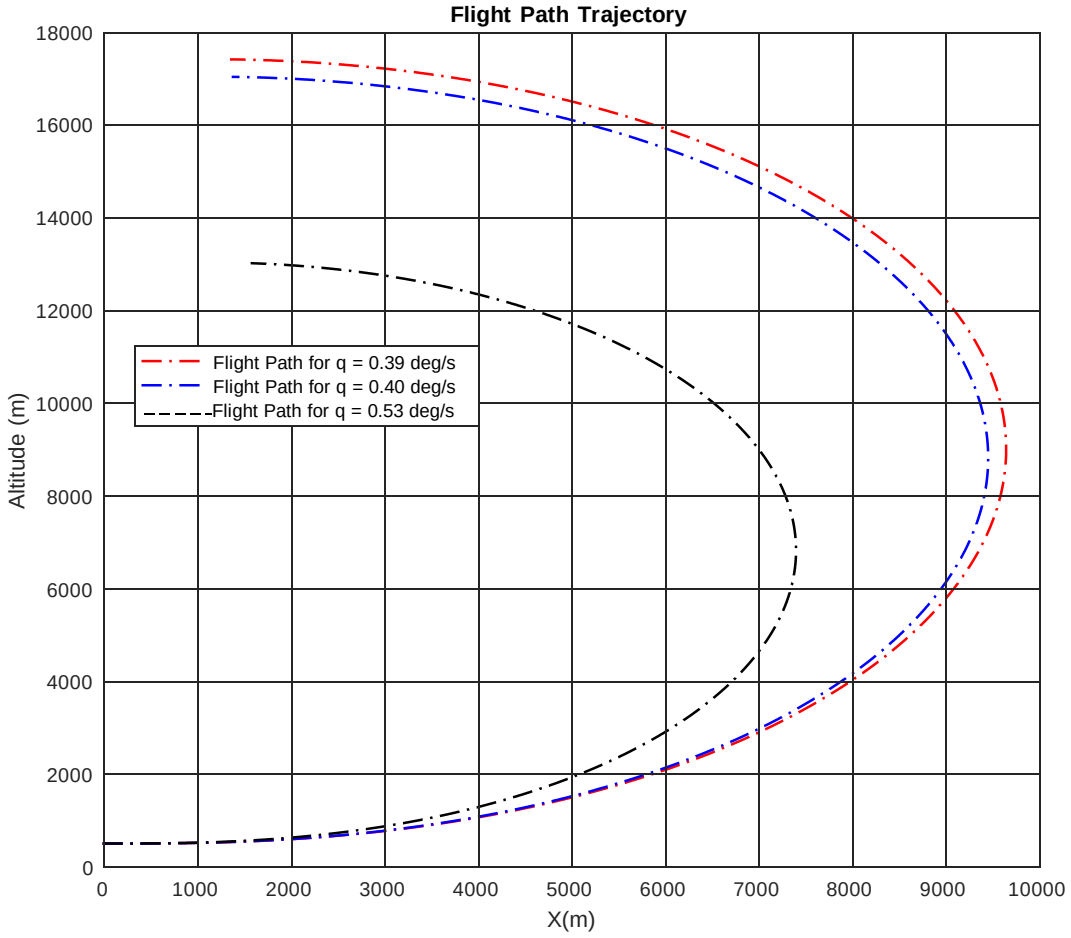

FIGURE 3.10: Flight path trajectory for different pitch rates at $V = 60$ *m/s*

3.5.3 Case II: Velocity (V) = 40 m/s

A similar approach is carried out for optimising the pitch rate for a flight velocity of $V =$ 40 m/s, setting in all the constraints to the problem algorithm discussed in Table3.3. The states obtained from the airplane dynamics, and the change in the pitch rate when subjected to these constraints are enumerated graphically below.

(a) Limiting Constraint : AOA α

With the flight velocity dropping to $V = 40$ m/s, which is around the stall speed of the aircraft,the first limiting constraint to hit the ceiling comes out to be the AOA at$\alpha =$ 6 deg. The dynamic responses of the variation of the states have been recorded

graphically in the Fig3.11. The optimised pitch rate obtained in this case is q = 0.12 deg/s.

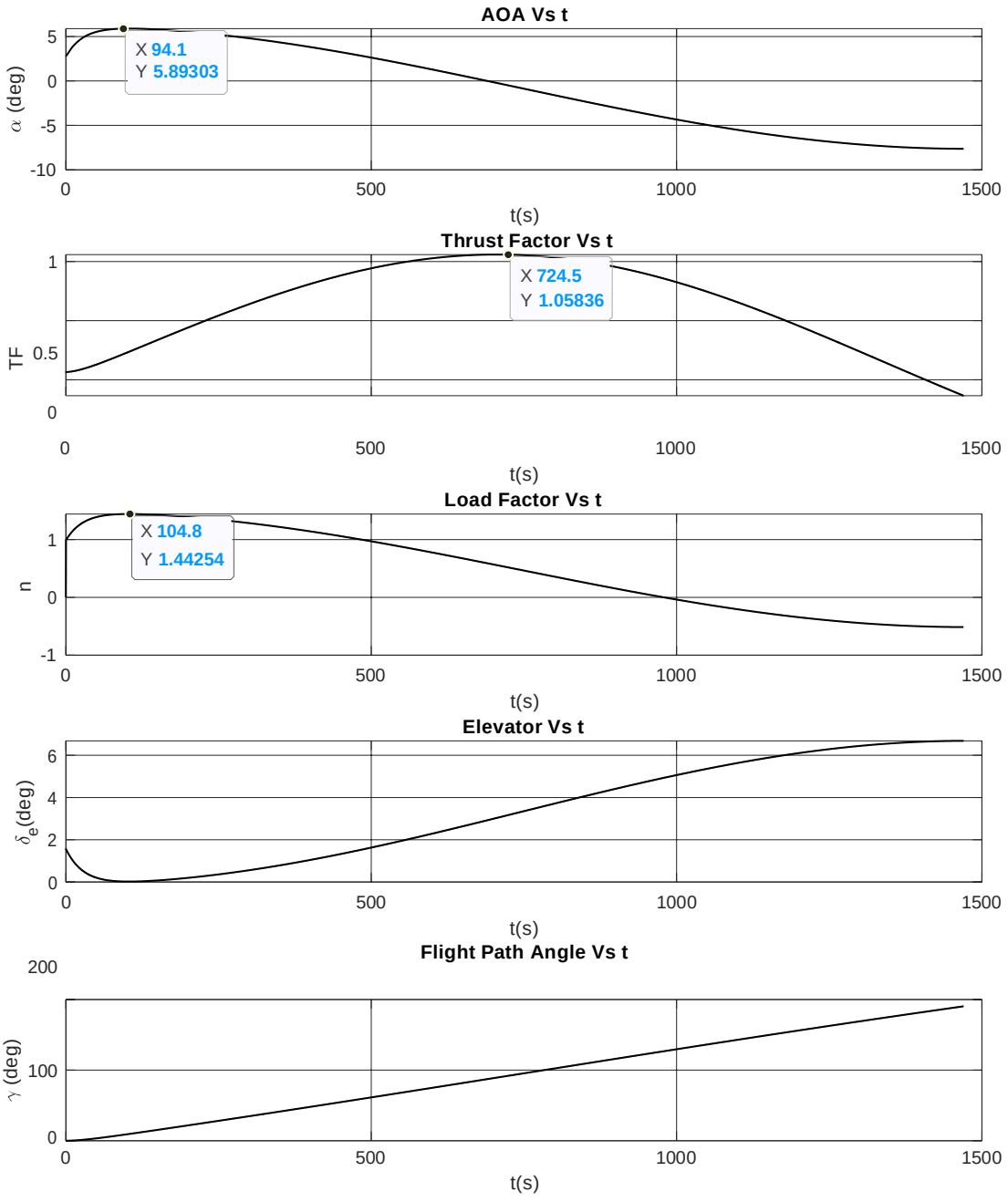

FIGURE 3.11: Variation of AOA, Thrust factor, Load factor, elevator and flight path angle with time

(b) Limiting Constraint : Thrust Factor

If we now relax the AOA restriction to the problem statement, we obtain the optimised pitch rate as q = 0.79 deg/s because of limiting thrust factor. However, this

is a theoretical simulation as because the AOA in this pull-up goes to as high as α = 21.52 deg, which is much beyond the stall limits of the airplane. The plots for this case has been presented in Fig3.12.

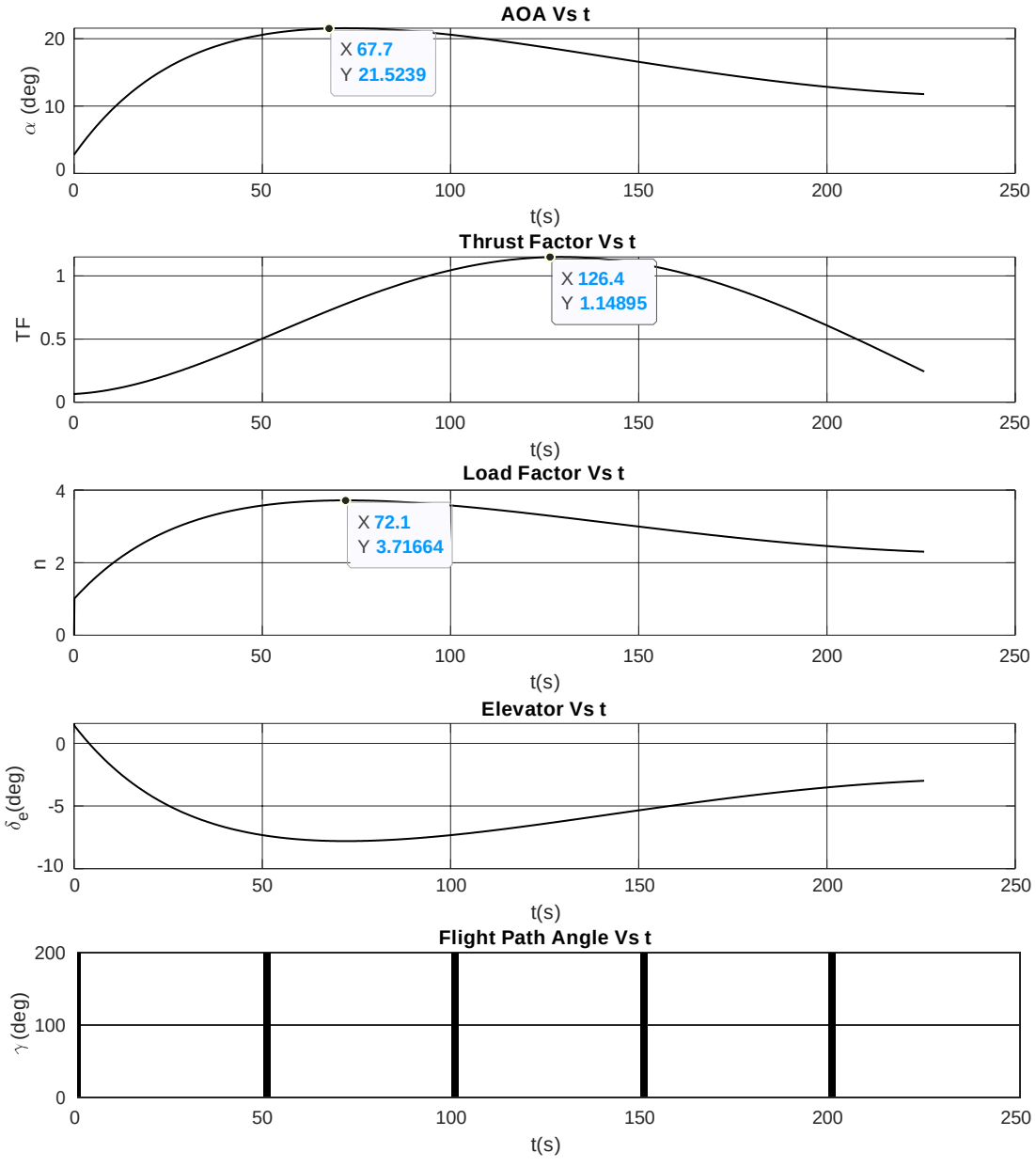

FIGURE 3.12: Variation of AOA, Thrust factor, Load factor, elevator and flight path angle with time

(c) Limiting Constraint : Load Factor

For the purpose of understanding the dynamics of this airplane, if we only enforce the load factor constraint and do away with the Thrust and AOA limitation, we obtain the results as plotted in Fig3.13. This hypothetical simulation results in an optimised pitch rate of q = 0.88 deg/s.

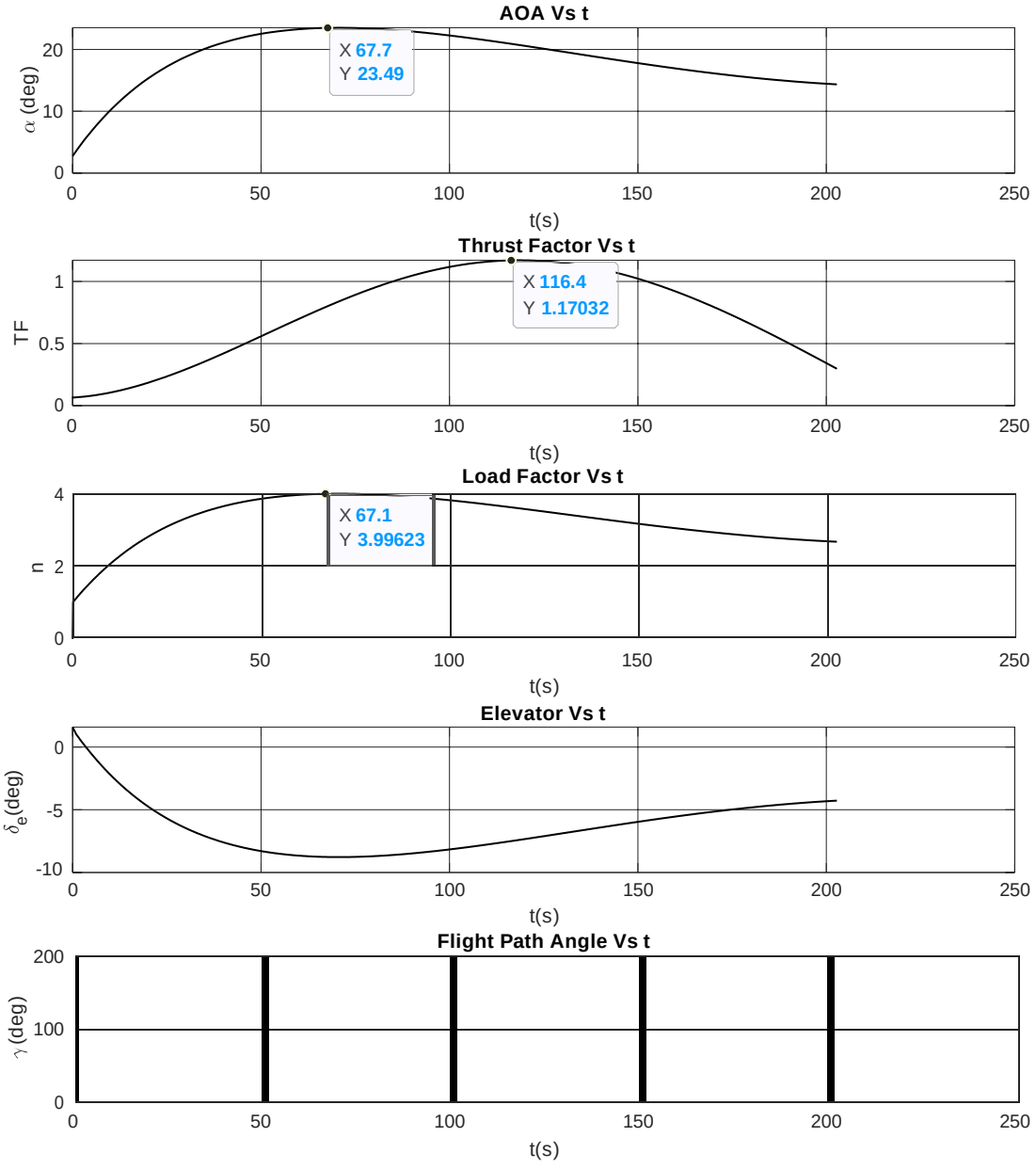

FIGURE 3.13: Variation of AOA, Thrust factor, Load factor, elevator and flight path angle with time

(d) **Flight Path Trajectory** The flight path trajectory plotted in Fig3.14, shows a comparative view of the aircraft profile in a pull-up maneuver at different pitch rates and at a velocity of $V = 40$ m/s.

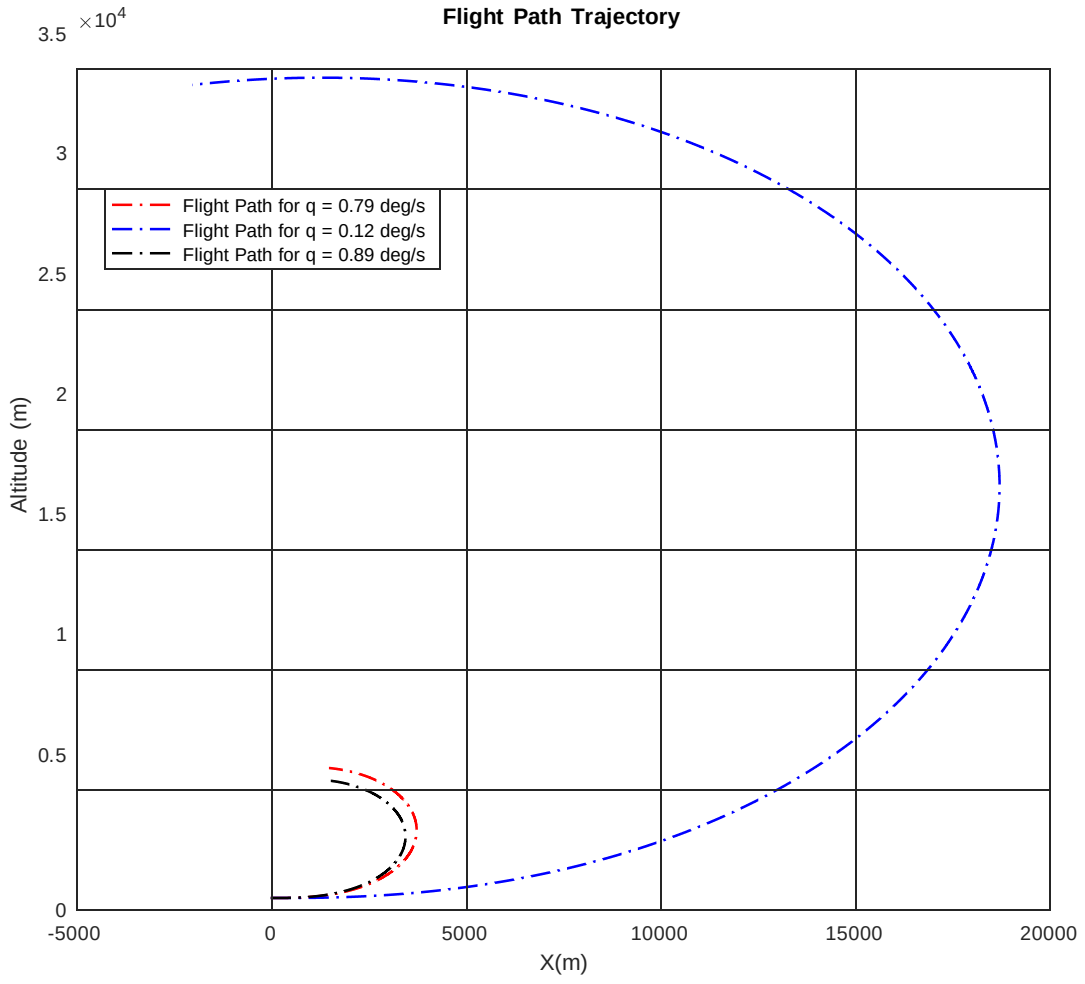

FIGURE 3.14: Flight path trajectory for different pitch rates at $V = 40$ *m/s*

3.6 Summary

The above analysis helped us understand the aerodynamic model of the Hansa-3 aircraft, its behaviour in the level trim state and also its dynamic response in the steady longitudinal pull-up maneuver. However, the main purpose of this study is to optimise the pitch rate of an airplane having a linear aerodynamic model across the entire bandwidth of AOA.

Although many parameters set as here as constraints were hypothetical, as brought out in the assumptions, but nonetheless it showed us the dynamic responses under various flight constraints exhibited by airplane having such fixed aerodynamic models.

The optimisation problem also helps us in finding the corner velocities given an aerodynamic model of the aircraft. This will help us in formulating $V - n$ diagrams and to better understand the operating envelope of the aircraft.

Chapter 4

Steady Longitudinal Pull-up Analysis : F-18 HARV

The F-18 HARV is a NASA High Angle of attack Research Vehicle, whose development has been inspired from the McDonnell Douglas F/A-18 Hornet. Unlike Hansa-3, this aircraft is an extremely maneuverable fighter which operates across a very wide span of AOA. The idea behind choosing this for our analysis was to comprehend its dynamics and to study the pitch optimisation behaviour for an aircraft whose aerodynamic model varies as a function of AOA.

Apart from the conventional control surfaces, this aircraft has thrust vectoring control which augments its super maneuverability and helps it to operate at high AOA.

4.1 Technical Specifications

(a) Control Surface Limits

The positional limits of F-18 HARV's primary control surfaces are as tabulated below in Table4.1:

TABLE 4.1: Control surface limits.

Control Surface	Symbol	Positional Limits
Rudder	δr	-30°, 30°
Elevator	δe	-25°, 10°
Aileron	δa	-35°, 35°

(b) Aircraft Characteristics

The geometric parameters of the aircraft is as tabulated below in Table4.2:

TABLE 4.2: Aircraft characteristics.

Parameter	Symbol	Value
Mass	m	16463 kg
Wing Span	b	11.4131 m
Aspect Ratio	AR	3.49
Mean Aerodynamic Chord	$\bar{c}$	3.5136 m
Wing Area	S	37.21 m^2
Pitch Inertia	I_{yy}	239720.82 kg-m^2
Yaw Inertia	I_{zz}	259969.95 kg-m^2
Roll Inertia	I_{xx}	30897.73 kg-m^2
Product of Inertia	I_{xz}	-2.6 kg-m^2

4.2 Aerodynamic Model

The aerodynamic modelling of the airplane defines the mathematical models which describe the aerodynamic forces and moments acting on the aircraft. The aerodynamic characteristics of each aircraft is unique and can be represented as a function of different state and control variables and its aerodynamic stability and control derivatives, as represented by set of Equations4.1. The F-18 HARV has a non-linear aerodynamic model whose parameters change as a function of its AOA, unlike the previous case of Hansa-3. Since we are focusing on longitudinal dynamic maneuvers, only the longitudinal aerodynamic model is used [7][2].

$$
\begin{aligned}
C_L &= C_{L_{comb}} + C_{L_q} \frac{q\bar{c}}{2V} + C_{L_{\delta e}} \delta e \\
C_D &= C_{D_{comb}} + C_{D_q} \frac{q\bar{c}}{2V} + C^{D_{\delta e}} \delta e \\
C_m &= C_{m_{comb}} + C_{m_q} \frac{q\bar{c}}{2V} + C_{m_{\delta e}} \delta e
\end{aligned}
\tag{4.1}
$$

The static variation of the coefficient of lift C_L, coefficient of drag C_D and the coefficient of pitching moment C_m with the angle of attack α is graphically represented below, with the static longitudinal aerodynamic model given as

$$\begin{aligned} C_L &= C_{L_{comb}} \\ C_D &= C_{D_{comb}} \\ C_m &= C_{m_{comb}} \end{aligned} \tag{4.2}$$

(a) Lift Coefficient

The variation of coefficient of lift C_L with the angle of attack, for a range of α from -14 deg to 90 deg is plotted in Fig4.1. The curve is non-linear with a varying slope across the entire range of α. The C_{L_o} can be seen from the plot as -0.031.

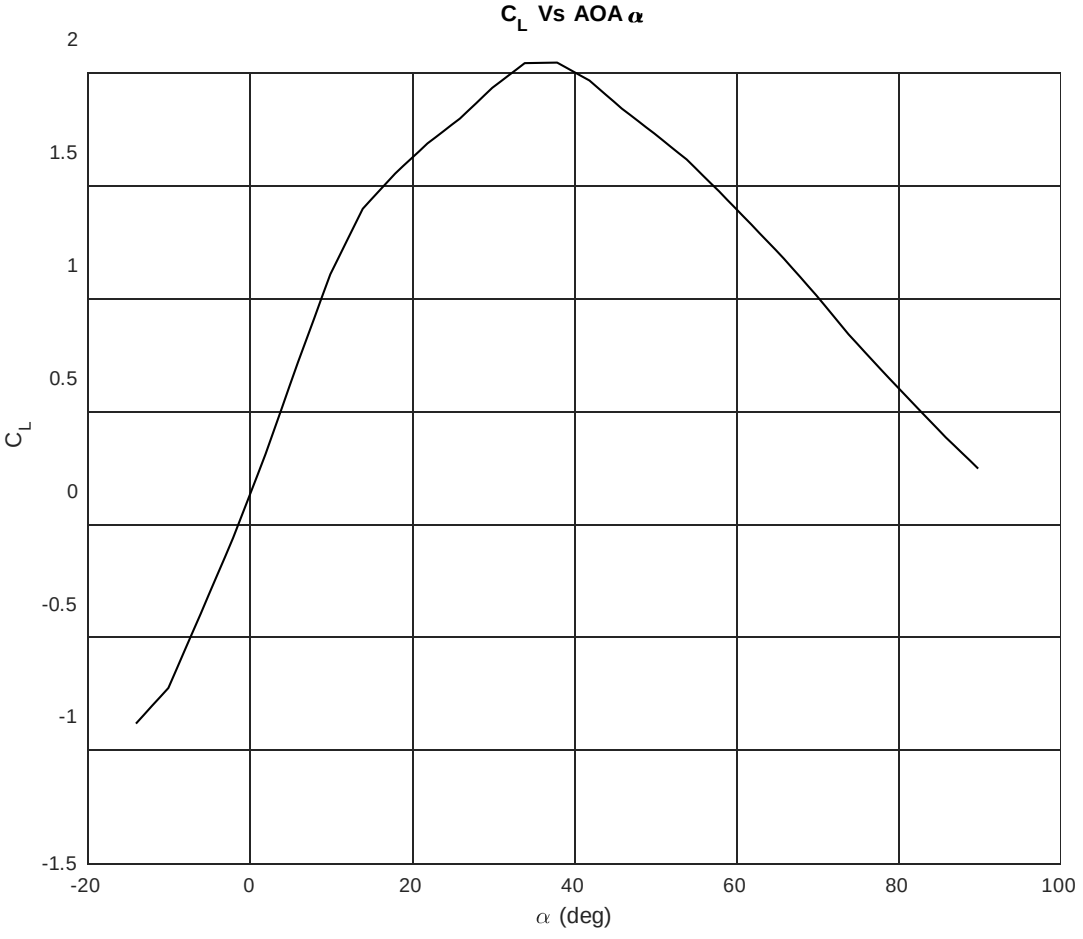

FIGURE 4.1: Variation of C_L Vs α

(b) Drag Coefficient

The variation of coefficient of drag C_D with the angle of attack for a range of α from -14 deg to 90 deg is graphically represented in Fig4.2and it has a non linear curve as shown owing to the changing slope across the entire range of α. The value of the C_{D_o} is 0.03.

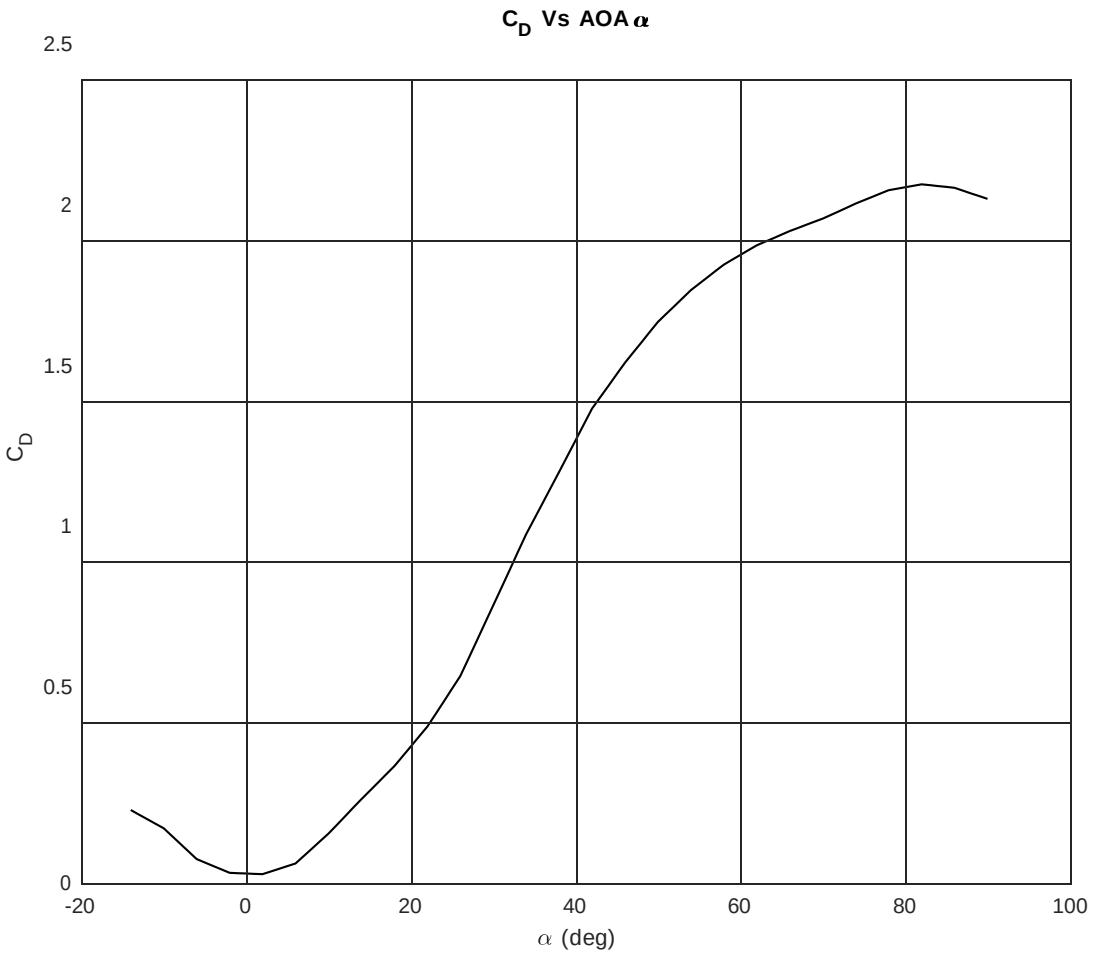

FIGURE 4.2: Variation of C_D Vs α

(c) Moment Coefficient

The variation of coefficient of pitching moment C_m with the angle of attack, for a range of α from -14 deg to 90 deg is plotted in Fig4.3. The plot is non linear due to the varying slope across the entire range of α and the C_{m_o} can be seen as 0.02.

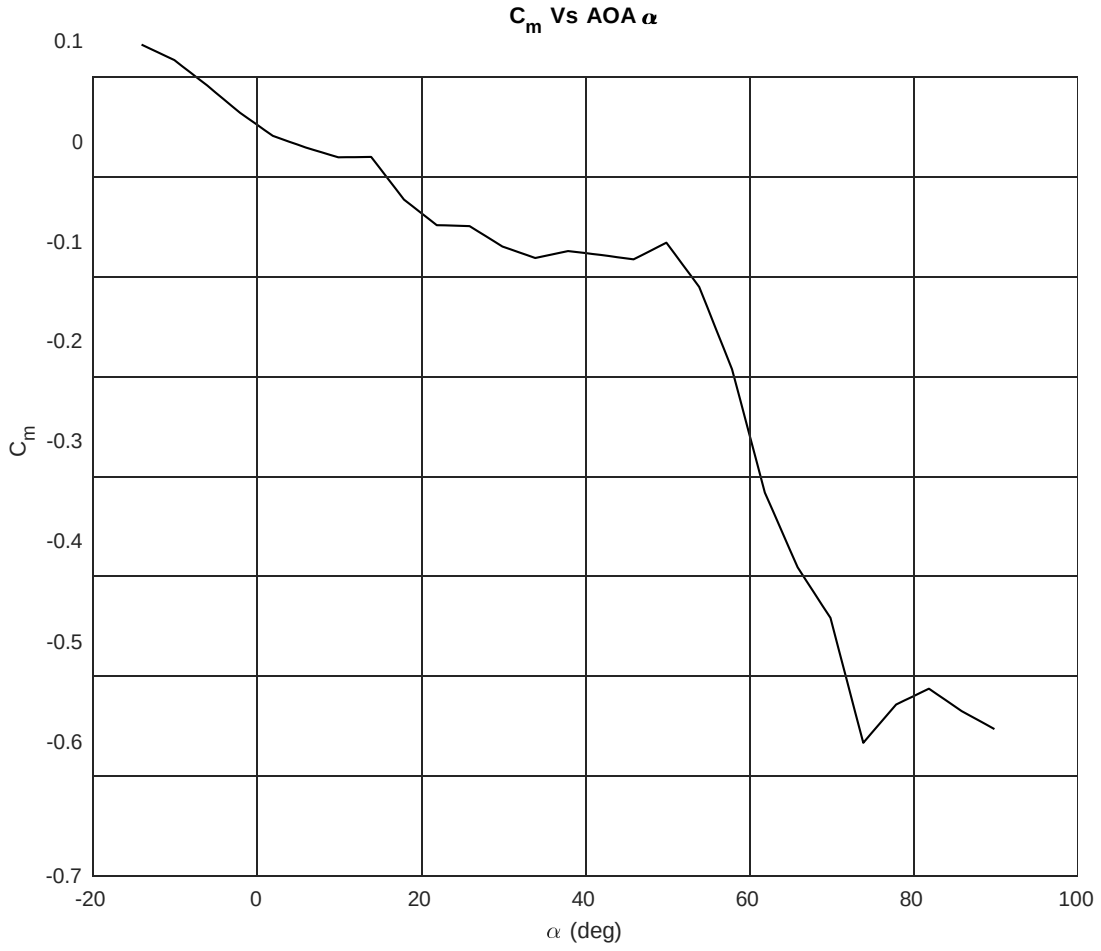

FIGURE 4.3: Variation of C_m Vs α

4.3 Assumptions

The mathematical model of F-18 HARV has aerodynamic parameters varying as function of AOA and hence the study of its pitching characteristics in the longitudinal plane would help us comprehend its complex dynamic behaviour. However, this analysis has been madeby considering a few assumptions as stated below:

(a) The F-18 HARV aircraft has a maximum thrust rating of 71.2 kN from each of its aero-engines, which amounts to 142.4 kN of thrust from its twin engines. However, here we have considered a limit thrust factor ($TF = T_{max}/W$) of 1.18 for setting the thrust limitation in the optimisation problem. The effect of thrust vectoring control is not considered here.

(b) The aircraft has a non linear curve of C_{L_α} across the entire range of AOA. The stall AOA can be apprehended from the plot in Fig4.1to be 40 deg approximately. This limit for AOA have been considered while setting the constraints in the problem statement.

(c) The load factor (n) has been approximated to be bound within the range $-2 \leq n \leq 6$ and the same has been used to set the constraint boundaries in the problem.

(d) The maximum all up weight ($W = m * g$) has been considered for defining the problem statement, where mass m = 16463 kg and acceleration due to gravity g = 9.81 m/s^2.

(e) Sea level altitude has been considered for calculating the air density ρ = 1.225 kg/m^3 for the entire computation.

4.4 Trim Analysis : Steady, Straight and Level

The level trim analysis of the F-18 HARV becomes vital for our study, because it is this steady state condition which acts as the starting point for the steady pull-up optimisation problem. The equations governing this state have been defined in Equations3.3.

The steady state level trim analysis for this aircraft has again been carried on two flight velocities as illustrated below in two separate cases.

4.4.1 Case I: Velocity (V) = 220 m/s

The dynamic response of the airplane when it is trimmed at straight and level conditions at flight velocity V = 220 m/s can be interpreted by analysing its states as graphically represented.

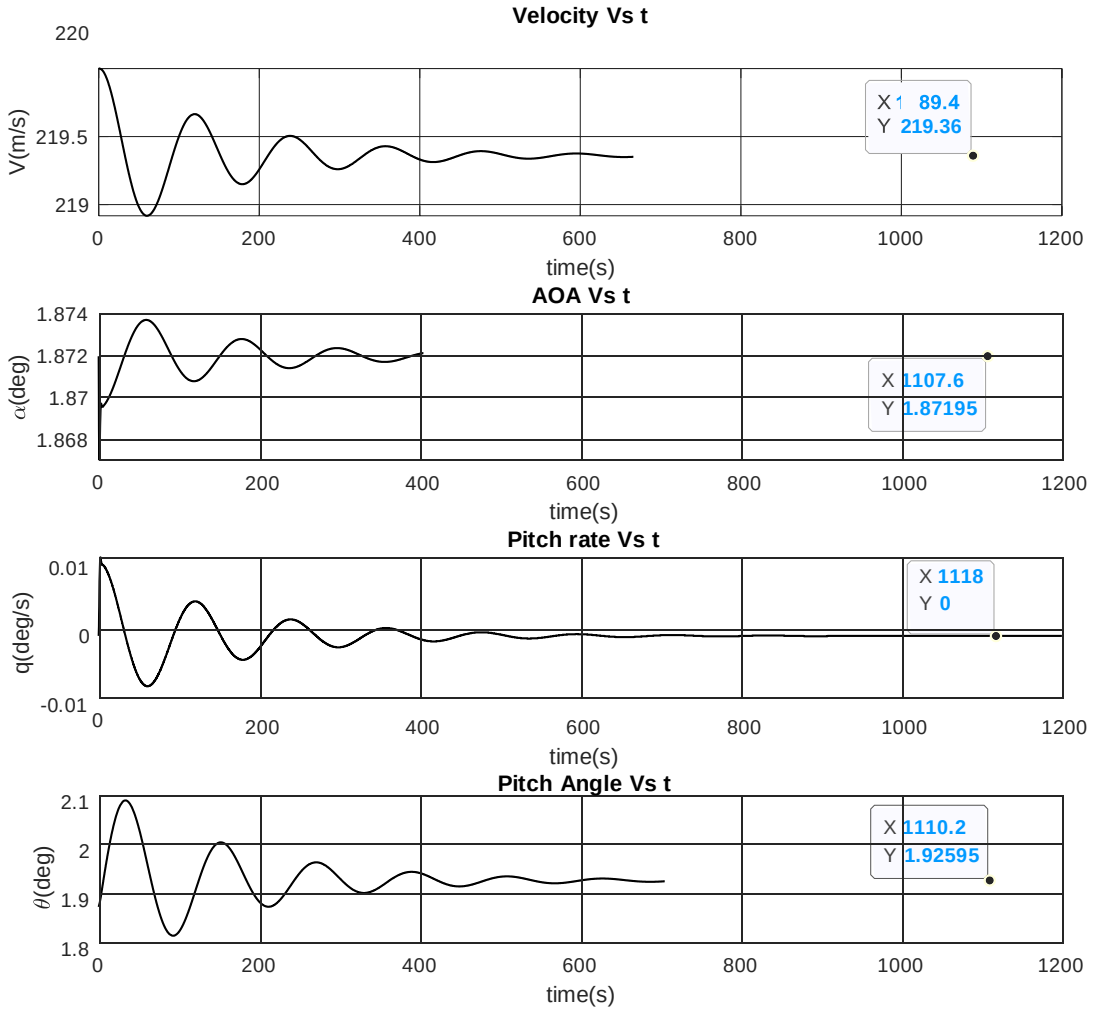

FIGURE 4.4: Velocity, AOA, pitch rate and pitch angle at level trim state

The velocity, AOA, pitch rate and the pitch angle settles down at V = 219.4 m/s, α = 1.88 deg, q = 0 deg/s and ϑ = 2.07 deg respectively as seen from Fig4.4. The control inputs corresponding to the level trim state are elevator δ_e = 0.367 deg and thrust T = 28733 N.

4.4.2 Case II: Velocity (V) = 150 m/s

Similarly, the response of the airplane when it is trimmed at flight velocity V = 150 m/s can be seen in Fig4.5. The velocity, AOA, pitch rate and the pitch angle finally settles down at V = 149.4 m/s, α= 3.57 deg, q= 0 deg/s and ϑ = 3.6 deg respectively. The

control inputs corresponding to the level trim state are elevator δ_e = 0.032 deg and thrust T = 21030 N.

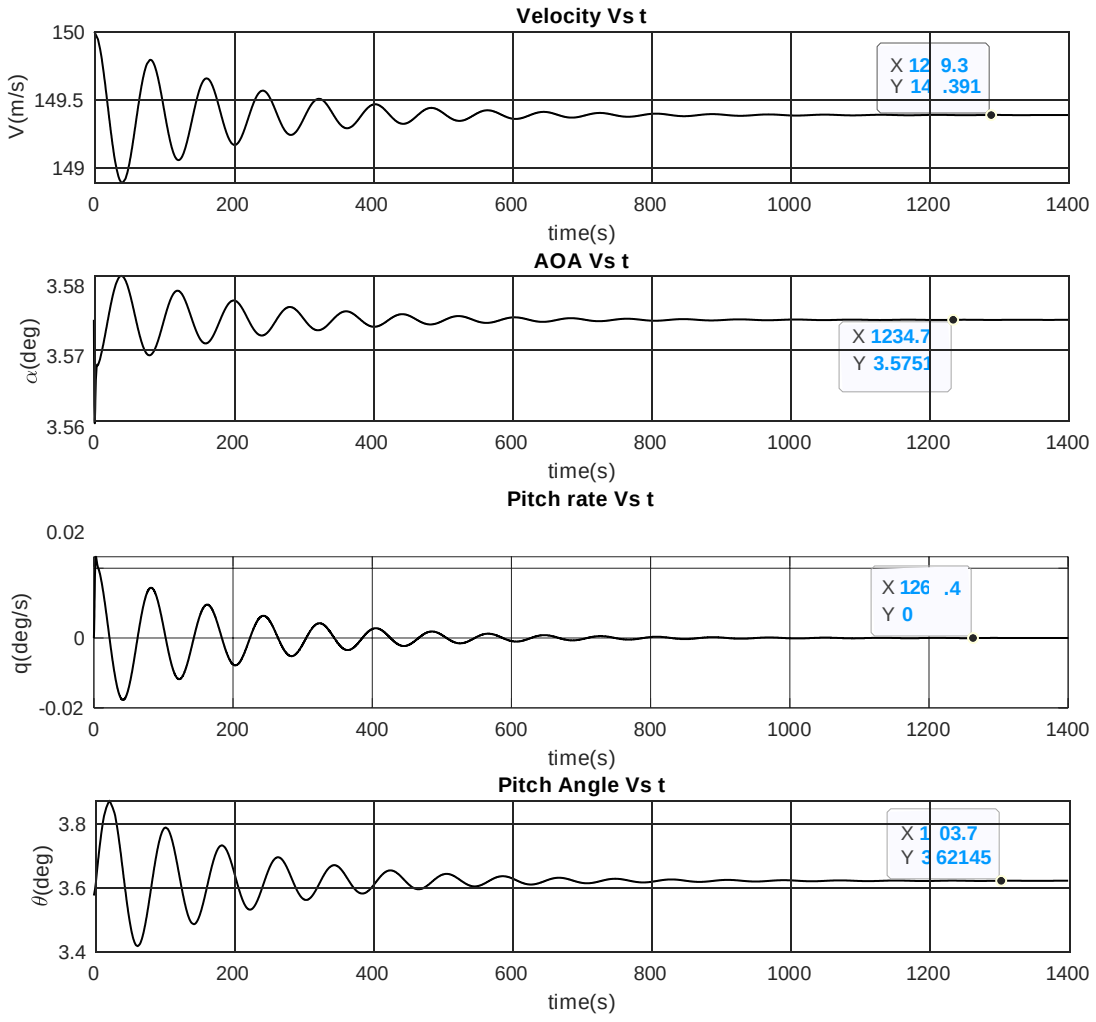

FIGURE 4.5: Velocity, AOA, pitch rate and pitch angle at level trim state

4.5 Trim Analysis : Steady Longitudinal Pull-up

A steady coordinated longitudinal pull-up is a symmetric maneuver carried out in the vertical XZ-plane where the airplane initiates the maneuver from a straight and level-trim flight with the flight path angle varying from γ = 0 deg to γ = 180 deg inverted state. Our point of interest is the dynamic response of the airplane during the entire maneuver till it settle downs in the γ = 180 deg state in the least possible time, all the while maintaining

a steady pitch rate. The steady state dynamic and kinematic equations governing this maneuver is shown below in Equation4.3. The airplane states are thereafter obtained by numerical integration of these equations using fourth order Runge Kutta method in MATLAB.

$$\dot{\alpha} = -\frac{\rho V S}{2m}\left[(C_{L_{comb}} + C_{L_q}\frac{q\bar{c}}{2V}) + (C_{D_{comb}} + C_{D_q}\frac{q\bar{c}}{2V})\tan\alpha\right] + \frac{\rho V S}{2m}\left[\frac{(C_{m_{comb}} + C_{m_q}\frac{q\bar{c}}{2V})(C_{L_{\delta_e}} + C_{D_{\delta_e}}\tan\alpha)}{C_{m_{\delta_e}}}\right] + \frac{g\cos\vartheta}{V\cos\alpha} + q$$

$$\dot{x} = V\cos\alpha\cos\vartheta + V\sin\alpha\sin\vartheta \tag{4.3}$$

$$\dot{z} = -V\cos\alpha\sin\vartheta + V\sin\alpha\cos\vartheta$$

$$\dot{\vartheta} = q$$

4.5.1 Pitch Rate Optimisation

Pitch rate optimization for steady pull-up, as discussed in the previous Chapter, helps to find the most optimal pitch rate while accounting for various constraints, by maximizing the defined cost function. In our problem statement, we define the cost function as the negative square of the pitch rate (q), wherein the flight path angle varies from $\gamma = 0$ deg to $\gamma = 180$ deg. Here the constraints that we set are Thrust factor ceiling, angle of attack α limitation and maximum attainable load factor (n). To solve this optimization problem, we have used MATLAB's *fmincon* function to arrive at the maximum attainable pitch rate within the bounds of the set constraints. The optimisation design for this problem statement is illustrated in the Table4.3.

TABLE 4.3: Design for pitch rate optimisation problem

Cost Function	$-q^2$
Guess Value	5 °/*s*
Constraints	**Limits**
Thrust Factor	1.18
AOA (α)	$-14° \leq \alpha \leq 40°$
Load factor(n)	$-2 \leq n \leq 6$

4.5.2 Case I: Velocity (V) = 220 m/s

The steady pull-up pitch rate optimisation is first carried out for a flight velocity of V = 220 m/s as per the design chalked out in Table4.3. The obtained states from the airplane dynamics are then enumerated graphically below. Herein, we initially applied all the constraints of thrust factor, AOA limit and load factor tolerance to the optimisation algorithm and thereafter have relaxed them, one at a time, as and when they were hitting the ceiling limit to appreciate the airplane pitching dynamics better.

(a) Limiting Constraint : Thrust Factor

The Fig4.6shows the variation of AOA, thrust factor, load factor, elevator deflection (δ_e) and flight path angle γ with time, wherein we can see that the limiting factor is thrust factor hitting the limit of 1.18. The maximum optimised steady pitch rate in this case is q = 4.67 deg/s.

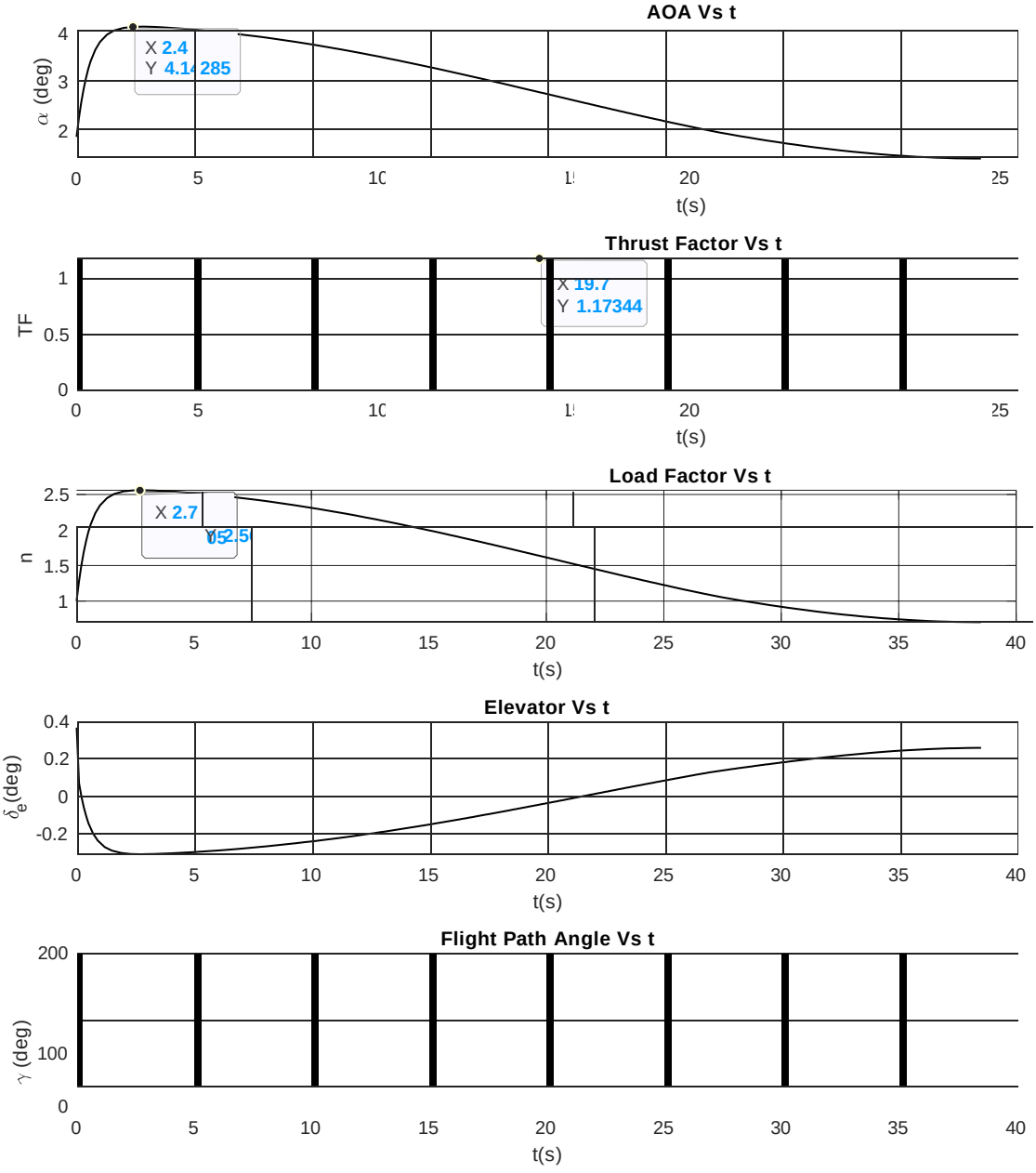

FIGURE 4.6: Variation of AOA, Thrust factor, Load factor, elevator and flight path angle with time

(b) Limiting Constraint : Load Factor

Again if we do away with the thrust restriction on the optimisation problem, the pitch rate gets furthermore enhanced to q = 16.18 deg/s, within the bound of the limiting load factor of n = 6. The plots of the dynamic responses in this case is brought out in Fig4.7.

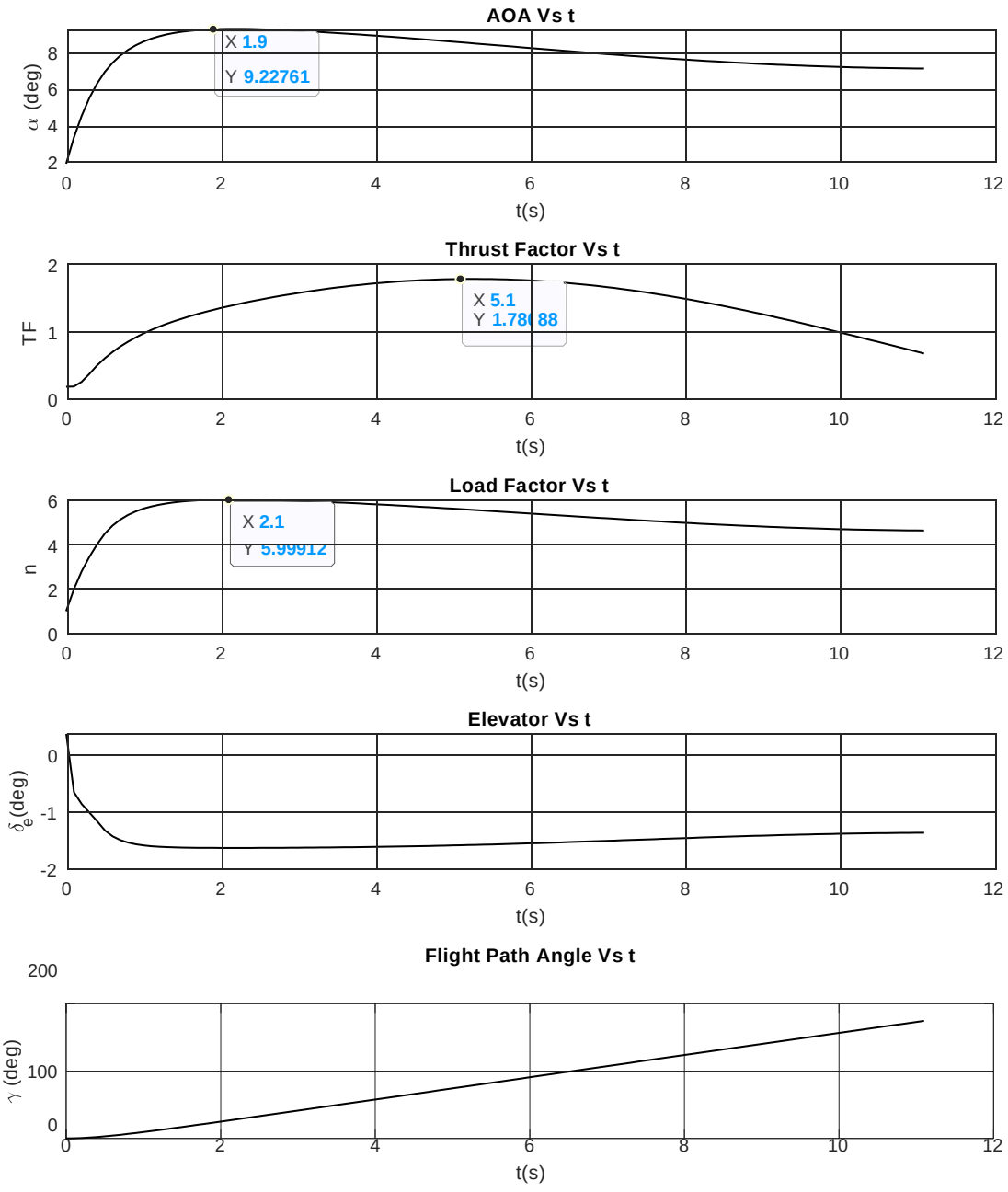

FIGURE 4.7: Variation of AOA, Thrust factor, Load factor, elevator and flight path angle with time

(c) Flight Path Trajectory

The flight path trajectory plotted in Fig4.8, compares the profile of the pull-up maneuver for the two cases at different pitch rates and at a velocity of $V = 220$ m/s.

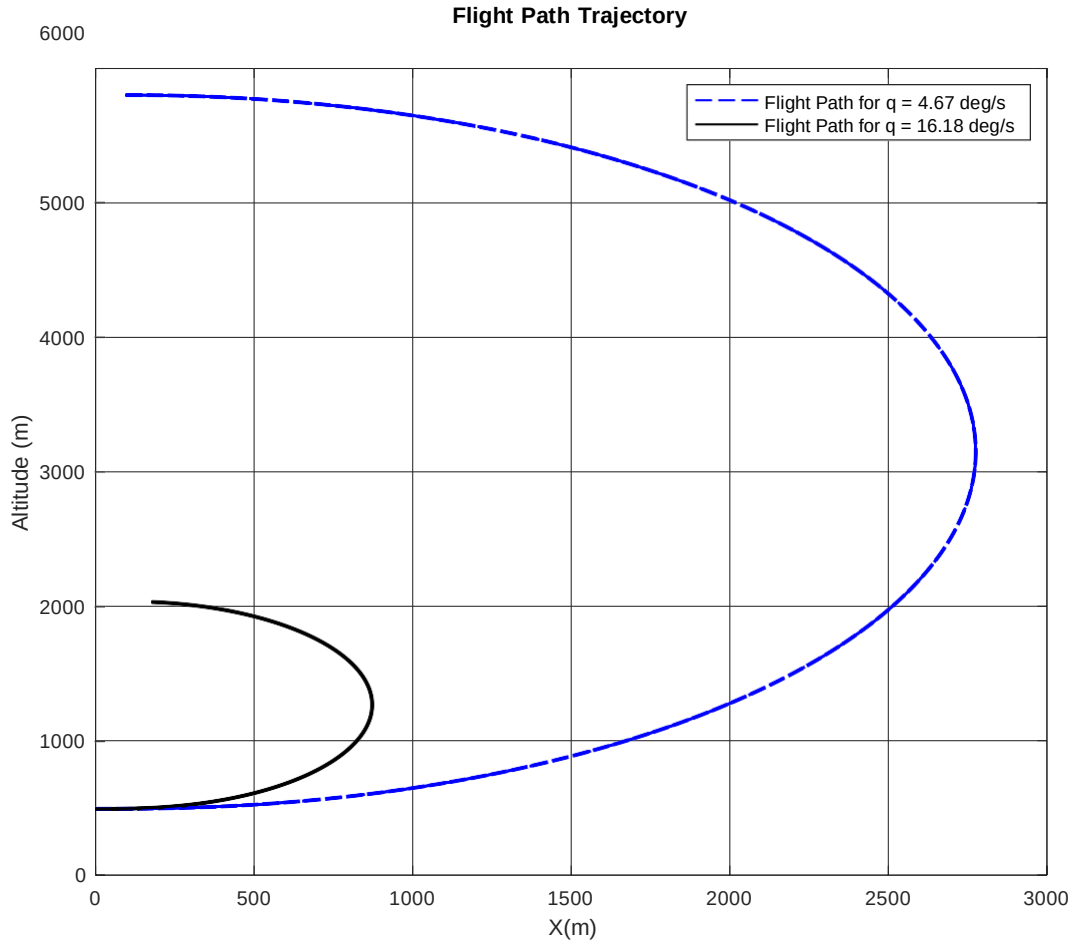

FIGURE 4.8: Flight path trajectory for different pitch rates at $V = 220$ *m/s*

4.5.3 Case II: Velocity (V) = 150 m/s

A similar approach is carried out for optimising the pitch rate for a flight velocity of $V =$ 150 m/s, setting in all the constraints to the problem algorithm discussed in Table4.3. The states obtained from the airplane dynamics, and the change in the pitch rate when subjected to these constraints are enumerated graphically below.

(a) Limiting Constraint : Thrust Factor

With the flight velocity dropping to V = 150 m/s, the first limiting constraint to hit the ceiling is again the thrust factor. The aircraft dynamic responses have been recorded graphically in the Fig4.9. The optimised pitch rate in this case is $q = 6.76$ deg/s.

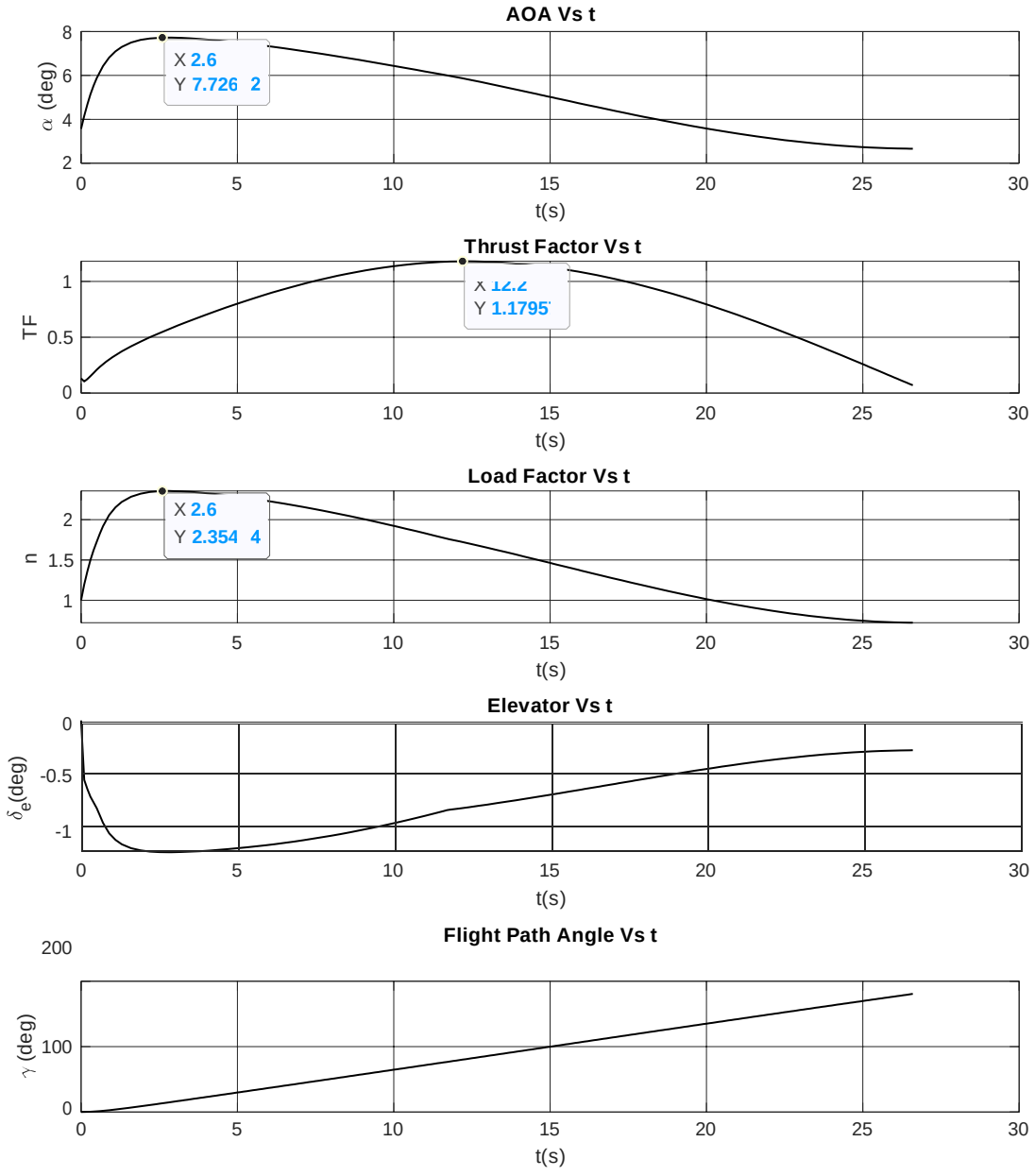

FIGURE 4.9: Variation of AOA, Thrust factor, Load factor, elevator and flight path angle with time

(b) Flight Path Trajectory

The flight path trajectory shows the aircraft profile in this pull-up maneuver at the constant pitch rate and velocity as shown in the Fig4.10.

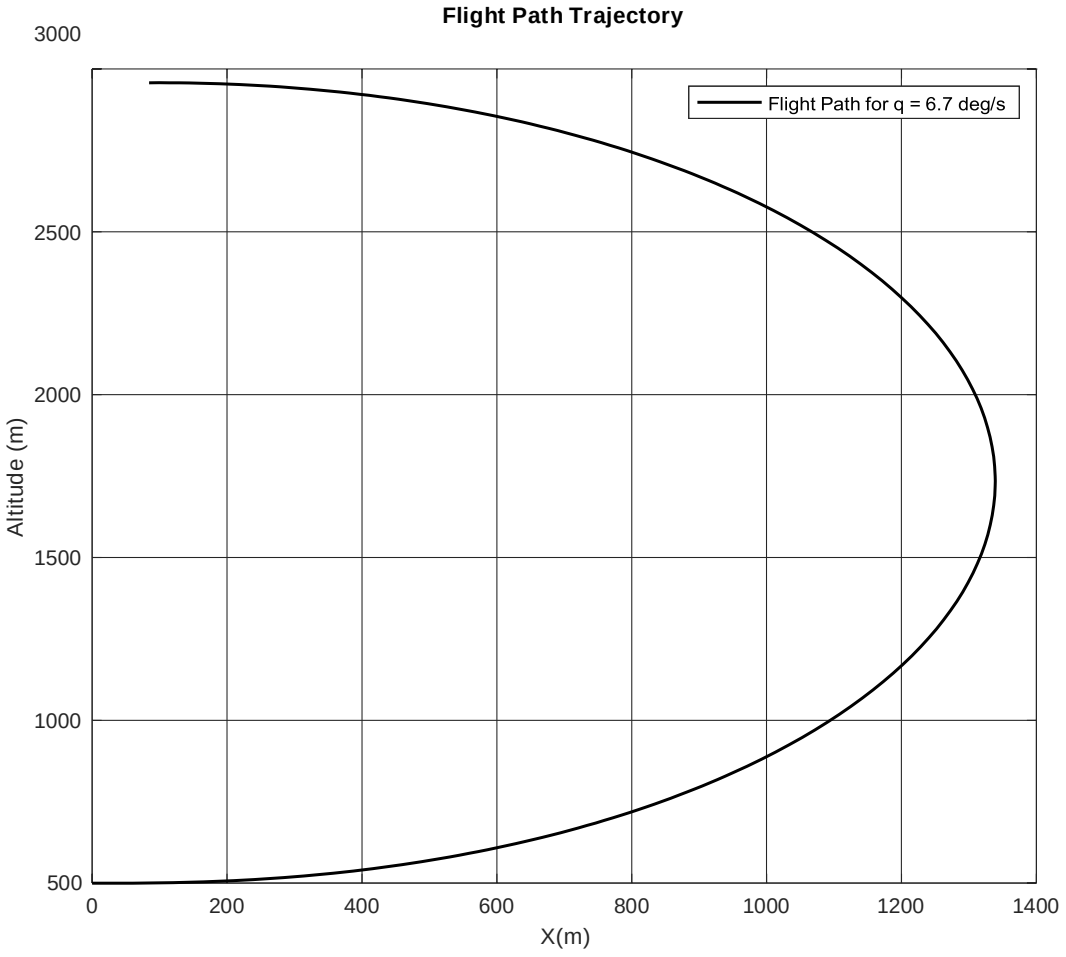

FIGURE 4.10: Flight path trajectory at $V = 150$ *m/s*

4.6 Summary

The above analysis helped us to understand the non-linear aerodynamic model of the F-18 HARV, its behaviour in the level-trim state and also its dynamic responses in the steady longitudinal pull-up maneuver. However, the main purpose of this study is to optimise the pitch rate of an airplane having a varying aerodynamic model across the entire bandwidth of AOA. Although we assumed the thrust factor limit as 1.18 while defining our problem statement, we could thereby explore the dynamic responses exhibited by such highly maneuverable fighter aircraft. The optimisation problem also helps us in finding the corner velocities given an aerodynamic model of the aircraft. This will help

us in formulating $V - n$ diagrams and to better understand the operating envelope of the aircraft.

It is interesting to note that while simulating the pitch rate optimisation for the two different flight velocities, the pitch rate obtained along with the thrust requirement seemedirrational when subject to the only constraint of AOA. The optimised results attained whensubjected to the only constraint of AOA in case of V = 220 m/s was q = 76 deg/s andat a required Thrust factor of 11.5, which was way beyond the aero-engine's capability. Similarly, for flight velocity V = 150 m/s, when subject to constraints of Load Factorand AOA, we obtained no viable solution for pitch rate. Thus, this process would helpus understand the airplane characteristics in the longitudinal plane. To understand the aircraft dynamics still better, similar exercises can be done in the lateral-directional plane for both steady and unsteady maneuvers.

Chapter 5

Conclusion and Future Scope

The study helped us understand the dynamic behaviour of the two aircraft having contrasting aerodynamic models. While the Hansa-3 exhibited a linear model, the F-18 HARV had an aerodynamic model with the parameters varying as a function of AOA. Thus our endeavour to optimise the pitch rate in a steady longitudinal symmetric pull-up maneuver for both the aircraft, gave us an insight into the stark difference in their dynamic responses and results. Although, at the outset we had made a few assumptions, with regards to the engine thrust ratings, the intention was to exploit their dissimilar aerodynamic models by entailing them into the dynamic maneuvers and drawing comparisons between them.

We however, do acknowledge the fact the Hansa-3 aircraft has not been designed to perform such inverted pull-up maneuvers, because of the power rating constraints of the aero-engine. These are primarily used by the flying clubs for imparting flying training and for joy rides, wherein they do not necessarily need to perform such acrobatic maneuvers. But this simulations can form a basis for understanding the dynamic responses of such aircraft when performing such high intensity exercises, the cognizance of the extra thrust requirement for such maneuvers, the load factor limits need to do perform agile pull-ups and so on. This would help us envision the expansion of the operational flight envelope and to enhance its maneuverability of such similar class of aircraft.

The other airplane we studied was comparatively highly agile and maneuverable and has been used by NASA for their high angle of attack research work. The F-18 HARV had a

non-linear variation of the aerodynamic parameters with AOA. This aircraft, undoubtedly had a high optimised pitch rate in the said maneuver when tested at two different flight velocities. The understanding from the dynamic performance could help us acquaint better with such aerodynamic models and propel our research further into developing such indigenized advanced fighters with robust aerodynamic models, equipped with agility and super-maneuverability.

The thesis work undertaken here was to optimise the pitch rate in a steady longitudinal pull-up by defining a cost function and solving against some set constraints. Further inline, the pitch-rate optimisation in this pull-up maneuver can be enhanced by factoring in a variable pitch rate during the maneuver with an aim to attain flight path angle γ = 180 deg from γ = 0 deg in the minimum possible time. Additionally, the possibilities and advantages of undertaking a rolling pull-up can be exploited and analysed. The optimisation study can also be extended in the lateral-directional plane to cover maneuversin the entire spectrum of the operational flight envelope.

Bibliography

[1]B. Etkin and L. D. Reid, *Dynamics of flight: stability and control*. John Wiley & Sons, USA, 1995.

[2]R. C. Nelson *et al.*, *Flight stability and automatic control*, vol. 2. WCB/McGraw Hill New York, 1998.

[3]N. K. Peyada, A. Sen, and A. K. Ghosh, "Aerodynamic characterization of hansa-3 aircraft using equation error, maximum likelihood and filter error methods," in *Proceedings of the International MultiConference of Engineers and Computer Scientists*, vol. 2, 2008.

[4]R. Kumar and A. Ghosh, "Estimation of aerodynamic derivatives using neural network based method," *IFAC Proceedings Volumes*, vol. 47, no. 1, pp. 897–904, 2014.

[5]A. Kumar and A. K. Ghosh, "Anfis-delta method for aerodynamic parameter estimation using flight data," *Proceedings of the Institution of Mechanical Engineers, Part G: Journal of Aerospace Engineering*, vol. 233, no. 8, pp. 3016–3032, 2019.

[6] *Type Certificate for Hansa-3, DGCA : Govt. of India*, 2000.

[7]A. C. Paris, *Estimation of the Longitudinal and Lateral-Directional Aerodynamic parameters from Flight Data for the NASA F/A-18 HARV*. West Virginia University, 1997.

[8]J. D. Anderson and M. L. Bowden, *Introduction to flight*, vol. 582. McGraw-Hill Higher Education New York, 2005.

[9]P. Raghavendra, T. Sahai, P. A. Kumar, M. Chauhan, and N. Ananthkrishnan, “Aircraft spin recovery, with and without thrust vectoring, using nonlinear dynamic inversion,” *Journal of Aircraft*, vol. 42, no. 6, pp. 1492–1503, 2005.

[10]B. N. Pamadi, “Performance, stability, dynamics, and control of airplanes,” 2015.